

BULGARIAN ACADEMY OF SCIENCES
INSTITUTE OF ROBOTICS

Section "Robotics in Energy"

M.Eng. Petar Ivanov Petrov

**INFLUENCE OF LOAD ON REACTIVE POWER IN ASYMMETRIC AND
NON-SINUSOIDAL REGIMES**

DISSERTATION ABSTRACT

of a dissertation for the award of the educational and scientific degree "Doctor" in
professional direction 5.2. Electrical Engineering, Electronics and Automation

Scientific supervisor:

Prof. DSc Ilian Hristov Iliev

Sofia

2025

The dissertation has been discussed and scheduled for defense at an extended seminar of the "Robotics in Energy" at the Institute of Robotics – BAS.

The research for the dissertation was conducted at a factory for the production of starter batteries and an industrial plant for the production of soda.

The defense of the dissertation will take place in room 427, building 2, at the Institute of Robotics – BAS

The materials for the dissertation are available at the registry of the Institute of Robotics – BAS

Acknowledgments: I express my respect and gratitude to my academic advisor for the valuable guidance and practical recommendations during the creation of this dissertation.

Scientific jury:

1. Assoc. Prof. Dr. Eng. Petko Nikolov Nedyalkov - IR-BAS
2. Prof. PhD. Siya Valcheva Lozanova - IR-BAS
3. Assoc. Prof. Dr. Eng. Orlin Lyubomirov Petrov - Ruse University "A. Kanchev"
4. Prof. PhD. Ivan Petrov Petrov - VTU "Todor Kableshkov"
5. Assoc. Prof. Dr. Eng. Martina Raychinova Tomcheva - VTU "Todor Kableshkov"

Members of the reserve scientific jury:

1. Prof. PhD. Snejanka Petrova Kostova - IR-BAS
2. Prof. PhD. Ivan Stefanov Minin - MGU "St. Ivan Rilski"

Author: Petar Ivanov Petrov

E-mail: p_petrov1977@abv.bg

Title: Influence of load on reactive power in asymmetric and non-sinusoidal regimes

A. GENERAL CHARACTERIZATION OF THE DISSERTATION WORK

Relevance of the problem

In recent years, the implementation of new technologies in the construction and reconstruction of compensating systems has been focused on the following main areas:

- Use of high-tech dry or semi-dry capacitor banks (CB);

- Implementation of specialized CBs for heavy operating conditions ($\text{THDi} \geq 30\%$) in the case of polluted networks;

- Introduction of disturbing inductances in the case of polluted networks;

- Implementation of specialized compensating equipment for low voltage (LV) capacitive loads;

- Use of SF₆ (sulfur hexafluoride) contactors for MV capacitor banks;

- Use of powerful specialized power electronic switching modules when compensation for rapidly changing and dynamic loads is required;

- Implementation of microprocessor controllers with single-phase or three-phase voltage measurement. The former are used in networks without asymmetry (voltage or current), offering a more cost-effective solution;

- Use of microprocessor controllers with resonance protection to eliminate resonance processes;

- Use of controllers with optimized control modes to achieve equal average annual utilization of individual capacitor banks. This approach significantly extends the service life of compensating systems (CS), as the controller switches the least used CBs. This ensures the simultaneous depreciation of all components of the CS.

Aims and objectives of the dissertation

The aim of this dissertation is as follows:

To investigate and analyze the processes of reactive load compensation under asymmetric and nonlinear regimes and at different load levels, to apply innovative computational and technological methods for rationalization and optimization, and to test the results in suitable industrial sites, demonstrating the technical and economic effectiveness of the implemented solutions.

To achieve this goal, it is necessary to form and solve the following tasks:

1. To conduct an investigation of the widely used conventional methods for reactive load compensation in the country, with the aim of studying and explaining their operational characteristics, analyzing high-tech modern solutions for reactive load compensation, and demonstrating their application in the ESS of industrial sites;
2. To synthesize modern theoretical frameworks for the study, analysis, and application of methods for reactive load compensation, with object-oriented, methodologically grounded, and practically applicable characteristics;
3. To conduct a study of reactive load compensation under nonlinear and asymmetric loading using an adequately synthesized methodology, tested in a suitable site for research;
4. To explore the possibilities for optimizing reactive load compensation in a large industrial facility using synchronous motors and capacitor banks, by solving an optimization task based on the criterion "Minimum of Total Annual Cost," while demonstrating the electrical energy efficiency of the technological solution.

Methods of research

The dissertation is based on a large volume of experimental studies, with all data and measured quantities processed and analyzed using methods of mathematical statistics, experimental design theory, and other tools.

Testing of the work

A significant portion of the results of the work are presented in the dissertation and the author's publications.

Structure and volume of the dissertation

The dissertation is 179 pages in length, structured in 4 chapters, contains numerous formulas, 104 figures, 38 tables, 129 titles of references of which 84 in Cyrillic and 45 in Latin. In the abstract, the numbering of figures, tables and formulae corresponds to that of the thesis.

Throughout the dissertation, the main terms and operational definitions are presented with their abbreviations and designations. These are, accordingly, set out on a separate page at the beginning of the thesis for ease of reading.

B. Brief Summary of the Dissertation

CHAPTER ONE

LITERATURE REVIEW ON CONVENTIONAL AND HIGH-TECHNOLOGY METHODS FOR REACTIVE LOAD COMPENSATION

The listed unfavorable conditions due to low $\cos\varphi$ require the implementation of measures in the ESS of industrial sites to improve $\cos\varphi$. These measures should be carried out in two directions – improving $\cos\varphi$ without compensating devices (natural methods) and improving $\cos\varphi$ with the help of compensating devices.

All these factors suggest that capacitor banks (CB) will remain the main technical means for reactive load compensation for many years to come. This is confirmed by the following activities:

- The existing capacitor banks (CB) in Bulgaria, with an installed capacity of hundreds of MVar, number in the thousands, many of which have exceeded their operational lifespan. The majority of them are oil-filled, with high dielectric losses, operating inefficiently, and it is advisable to replace them with dry capacitor banks of polypropylene type.
- Unlike the status quo ten years ago, many renowned manufacturers of electrical equipment now have strong positions in our market, with almost all offering high-quality solutions for capacitor banks (CB)-based compensating systems (CS). The most popular of them are Schneider Electric, ABB, Siemens, Legrand, and others. Additionally, there are companies offering optimized price solutions, occupying a lower class – ZEZ Sliko, Italfarad, MKS, ChinT, and many others. Given the scale of Bulgaria, this creates significant economic interests and strong competition, leading to very favorable financial conditions for the production, implementation, and operation of CB-based compensating systems.
- The development of technologies, as well as the fact that Bulgaria, as a member of the European Union, has adopted regulatory measures concerning the quality and safety of electrical equipment, has established CB-based compensating systems as a cost-effective, reliable, safe, and environmentally friendly technical solution for compensation of the reactive loads (CRL). In times of crisis and reduced load, this classic solution, with easy, simple, and efficient operation, is increasingly preferred as a technical solution. In this regard, a key task for implementing companies is to add more functionality to these devices by integrating them into other highly technological systems, thus making them more effective and reliable.

1.1.1 Characteristics of compensation of the reactive loads (CRL) using capacitor banks (CB)

Transverse CRL

In this method, capacitor banks (CB) are connected in parallel to the elements in the network. It is primarily used for low voltage (LV) and medium voltage (MV) in industrial sites. The main purpose of cross-compensation of the reactive loads(CRL) (Fig. 1.6) is to improve $\cos\varphi$ and, secondly, to achieve voltage regulation. The power of single-phase and three-phase CBs is determined by the following expressions:

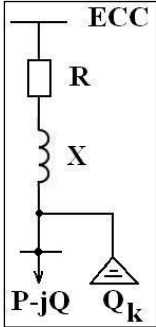


Fig. 1.6

$$Q = \omega C U^2 \cdot 10^{-3} [\text{kVAr}]$$

$$Q = \sqrt{3} \omega C U^2 \cdot 10^{-3} [\text{kVAr}]$$

where: U – phase voltage [V]; C – capacitor bank (CB) capacity [μF].

The active power losses before and after compensation of the reactive loads(CRL) (ΔP_1 и ΔP_2) and their reduction after CRL are determined by the following expressions:

$$\Delta P_1 = \frac{P^2 + Q^2}{U^2} R \cdot 10^{-3} [\text{kW}]$$

Longitudinal CRL

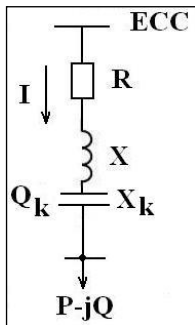


Fig. 1.7

In this method, capacitor banks (CB) are connected in series with the network, and the full current of the line passes through them. It is primarily used in high voltage (HV) networks to increase their stability, as well as in medium voltage (MV) networks in industrial sites, to improve the voltage regime (reducing voltage deviation and fluctuations).

Figure 1.7 shows the equivalent circuit for longitudinal CRL. The power of the CB is determined by the consideration that the current through it is equal to the full current I passing through the supply line [82]:

$$Q_K = \frac{I^2}{\omega \cdot c \cdot 10^{-3}} [\text{kVAr}]; I = \frac{U}{X_K} \cdot 10^{-3} [\text{A}]$$

Therefore, the power of the capacitor bank (CB) in longitudinal compensation (as opposed to that in transverse compensation) is a variable quantity that changes over time, depending on the changes in the load current in its line

1.2.1. Modern solutions for compensation of the reactive loads(CRL) based on flexible alternating current transmission systems (FACTS)

FACTS (Flexible Alternating Current Transmission Systems) were proposed in the late 1980s by EPRI (Electric Power Research Institute), USA, as a result of efforts to introduce and develop high-voltage direct current (HVDC) transmission systems with capacities ranging from hundreds to several thousand megawatts. HVDC

overhead lines with lengths of approximately 1000 km and cable lines around 50 km long for crossing sea straits or connecting electrical grids with different frequencies are equipped with so-called converters (transformers) to convert alternating current to direct current and vice versa. Currently, over 50 HVDC overhead and cable transmissions have been built worldwide, with a nominal voltage of 110 kV to 1500 kV, an overall transmission capacity of around 50,000 MW, and a converted power of 100,000 MW [127].

The rectifiers and inverters used in converter systems over the past decade have been built using controllable components – new-generation thyristors (GTO, IGBT, IGCT). Voltage Source Inverters (VSI) with pulse width modulation (PWM) have been realized with IGBT (Insulated Gate Bipolar Transistors) components. These have significantly advanced, reaching limits of 4.5 kV for voltage and 1.8 kA for current load. Such converters have significant advantages over traditional ones (such as our SVC installed at the “Dobruja” Substation): they do not require expensive filters for higher harmonics, nor do they need a source of reactive energy or an exchange of information between the two converters when dealing with HVDC transmission. *By generating voltages with a specified frequency and adjustable amplitude and phase, they represent real static devices capable of delivering or absorbing both active and reactive power, with high speed and sufficient reliability.*

The first high-voltage direct current (HVDC) transmission with new-type converters was implemented in 1998 in Sweden for transmitting 50 MW of electrical power via an underwater cable over a distance of 70 km from a wind farm in Gotland to a substation in the country’s main EEC. Shortly afterward, a similar link with a transmission capacity of 225 MW was established between Finland and Estonia. In May 2002, a high-voltage direct current transmission with a length of 40 km, a capacity of 330 MW, and a nominal voltage of 138 kV was commissioned between Connecticut and Long Island, USA.

Passive filters

In electrical networks, filters are primarily used to reduce the amplitude of current or voltage at one or more fixed frequencies (**parallel filters**). When it is necessary to prevent currents with a specific frequency from penetrating into certain nodes of converter stations or parts of the electrical system, serial filters can be used, consisting of parallelly connected capacitors and inductors that create a high resistance to the current at the selected frequency. However, such a solution cannot be used to limit the harmonics of the source itself, as the generation of harmonics by nonlinear elements is an inherent feature of their normal operation. As for the static converters themselves, measures are typically taken to limit the penetration of current harmonics into the system by creating short circuits with low resistance for the harmonic frequencies. In principle, it is possible to create combined serial and parallel passive filters to reduce current and voltage harmonics, although this results in significant losses of electrical power and requires substantial resources.

The **parallel filter** is tuned to a specific frequency if at that frequency its capacitive and inductive reactances are equal. The **quality factor** of the filter - Q , determines the accuracy of its tuning. Filters with a high quality factor have $Q = 30 \div 60$. Filters with a low quality factor have little resistance over a wide range, especially when $Q < 5$. If such a filter is tuned to the seventeenth harmonic, it can be considered a high-frequency filter.

Figures 1.17a, b, c, d show the basic diagrams of passive filters and their corresponding resistance-frequency relationships.

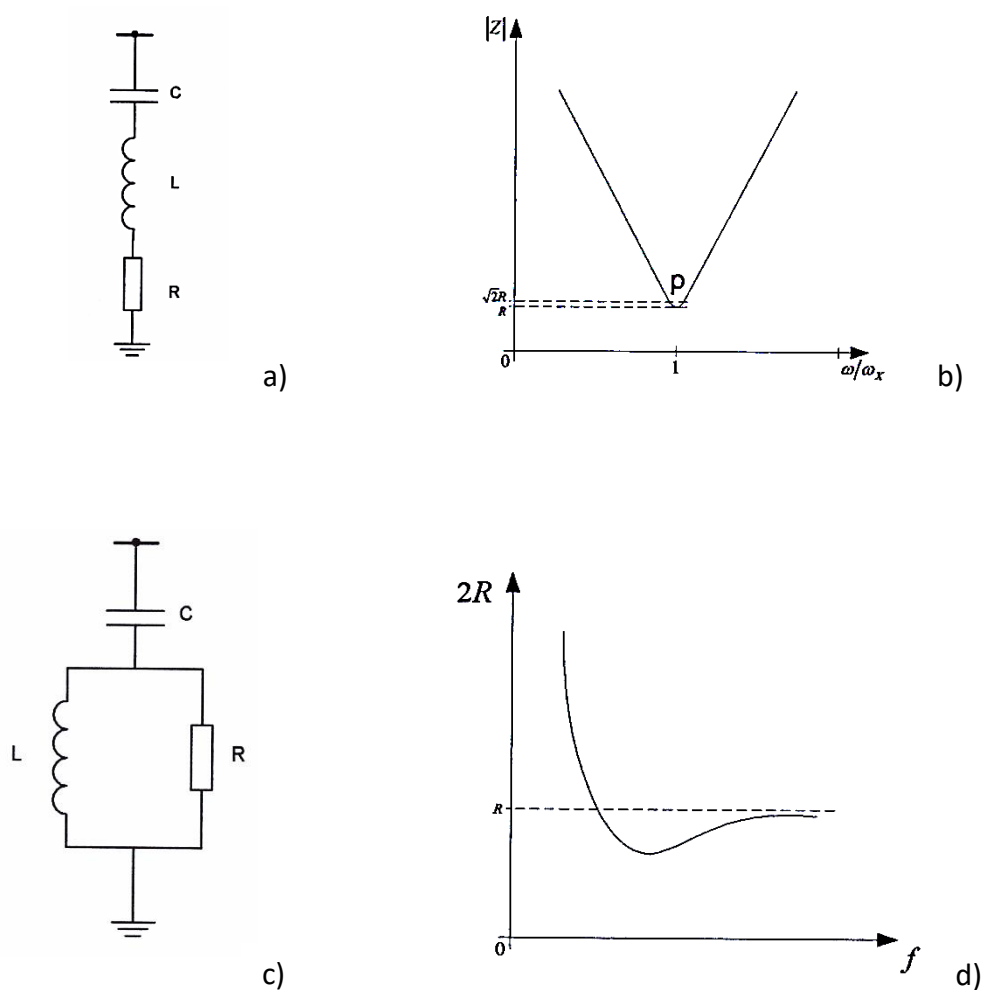


Fig.1.17 Diagrams and dependencies for passive filters

For a tuned filter, the quality factor is defined as the ratio of the inductive or capacitive reactance at resonance to its active resistance.

$$Q = \frac{X_0}{R} \quad (1.33)$$

As shown in Figure 1.17b, the bandwidth is limited by the frequency at which the reactive resistance of the filter is equal to its active resistance (i.e., the angle of the total resistance is equal to 45°), and the frequency of the total resistance is equal to $\sqrt{2}R$.

The quality factor is related to the bandwidth and is expressed by the following relationship:

$$Q = \frac{\omega_n}{p} \quad (1.34)$$

where: ω_n - the tuned frequency, rad/s ; p - bandwidth

The tuning accuracy of the filter and the attenuation of high frequencies are inversely proportional to the quality factor, i.e.

$$H = \frac{R}{X} \quad (1.35)$$

MAIN CONCLUSIONS AND RESULTS FROM CHAPTER ONE

1. *This chapter provides a detailed review of conventional methods for compensation of the reactive loads(CRL). These methods have found wide application in the ESS of industrial sites and the public utilities sector. Their study and understanding remain relevant due to their widespread use, despite the trends toward gradual abandonment. They are characterized by simplicity in operation during implementation, do not require highly qualified personnel for maintenance and repair, and have relatively low operational costs. Their longevity is further supported by the fact that the current energy sector in the country is not oriented towards the application of innovative technical solutions, due to misunderstandings and reluctance from administrative factors who do not recognize the benefits of implementing such technologies. The lag in this area compared to European standards is significant. To overcome this negative situation, measures are required, including changes in the regulatory framework and an overall strategy by regulatory bodies regarding the role of CRL in improving energy efficiency.*
2. *An analysis has been made of high-tech innovative technical solutions for compensation of the reactive loads(CRL), related to the application of circuit design setups based on power electronics, microprocessor modules, and computer systems. High-efficiency circuit solutions for synthesizing passive and active filters have been presented. The possibilities for achieving intelligent adaptive technical solutions with very high efficiency have been analyzed. Furthermore, the complex impact of filter-compensating systems has been explained, through which multiple parameters related to CRL are minimized simultaneously.*

CHAPTER TWO

MODERN THEORETICAL APPROACHES FOR STUDYING, ANALYZING, AND APPLYING METHODS FOR REACTIVE POWER COMPENSATION

2.1 Theoretical approach for determining the effective values of certain electrical quantities related to compensation of the reactive loads(CRL)

Asymmetric and nonlinear regimes in electrical systems are evaluated using two main approaches: Fourier harmonic analysis and the Fortescue symmetrical components method. In the 20th century, various researchers (Budeanu, Clark, Park, Akagi, Frize, Tolbert, Pent, etc.) developed the so-called Power Theories, which provide a new approach for evaluating different types of power, and consequently, new technical and technological solutions for compensation of the reactive loads(CRL). Several power theories are known, based on the use of instantaneous power, or the so-called "P-Q theories". Initially, they were developed for three-phase three-wire networks and later extended to four-wire systems with a neutral conductor.

The P-Q theory belongs to the theories in the time domain (as opposed to frequency domain theories, such as Fourier decomposition), which allows it to be used both for steady-state and transient regimes. This makes it one of the most commonly used theories for controlling active filters. The advantage of the theory is the simplicity of the calculations, which are based solely on arithmetic operations. The only exception is the separation of some components into constant and variable parts. Nevertheless, the theory enables the definition of regimes in any power supply system, achieving the determination of quantities within 1/6 to 1 period of the fundamental frequency. The essence of P-Q theory is a transformation from a stationary system with a-b-c coordinates into a system with α - β -0 coordinates. This corresponds to the algebraic transformation known as Clarke's transformation, where the α - β coordinates are orthogonal to each other, and the 0 coordinate corresponds to the components with zero sequence. The components of the zero sequence differ from the zero sequence components calculated using the symmetrical components method (Fortescue transformation).

In 1932, Fryze [10,12] extended the concept of the power triangle by developing it for non-sinusoidal conditions. The idea is to define an instantaneous current that matches the shape of the voltage waveform. This current $i_a(t)$ is called the instantaneous active current, and the product of the active current and the voltage (if it is purely sinusoidal) gives the active power of the load. The current component - $i_n(t) = i(t) - i_a(t)$, the difference between the full current and the active current was called by Fryze the

"wattless current." The integral of the product of the voltage and the reactive current is zero. As a result of this concept, Fryze concluded that an electrical load powered by non-sinusoidal voltage can be modeled by using linear conductance in parallel with a current source, whose current is equal to i_n . Fryze's model is mathematically correct and directly follows from the approach borrowed from sinusoidal linear systems. However, it is a simplified model that does not explore all the details of instantaneous power and does not reveal the true mechanism of energy transfer between the power source and the load. For a power theory to explain physical phenomena, it must originate from the electromagnetic field [18] and be based on the electric field vector \vec{E} and the magnetic field intensity vector \vec{H} . The cross product of these two vectors is known as the Poynting vector:

$$\vec{\Phi} = \vec{E} \times \vec{H} \left[\frac{W}{m^2} \right] \quad (2.1)$$

In [18], the application of these vectors in the study of electrical circuits is shown. Many of these studies are incorporated into the IEEE Std 1459-2010 standard, titled "*Definitions for the measurement of electric power quantities in sinusoidal, non-sinusoidal, balanced, or unbalanced conditions*" [19], which can serve as a basis for investigating different types of power or for studying power losses and compensation of the reactive loads(CRL) processes.

In Table 2.1, a comparison of different power theories is made depending on whether they use instantaneous or average values and on the phase characteristics of the supply [25]. They are classified into three categories:

- *Power theories defined in the time domain;*
- *Power theories defined in the frequency domain;*
- *Power theory based on an optimization approach [22] ;*

The Generalized Instantaneous Non Active Power (GINAPT) theory is based on Fryze's idea of non-active current power and is an extension of the theory proposed in [20]. It does not use Fourier transformation, and the quantities (currents, powers, etc.) are calculated based on instantaneous values. The analysis shows that, by neglecting the impedance of the supply lines, Fryze's definitions and those of the optimization approach fully coincide. All definitions are time-dependent and are presented in Table 2.2.

Table 2.1: Comparison between some power theories

Author(s) of power theory	Year of Publication	Number of phases in the system			Value of the quantities	
		1	3	Multi-phase	Average and/or effective values	Instantaneous Value
Power theories defined in the time domain						
Fryze (Fryze Power Theory) - orthogonal currents	1931	x			x	
Kusters and Moore - inductive and capacitive currents	1979	x			x	
Depenbrock - The first harmonic of voltage and current	1979	x			x	
Akagi, Nabae, Kanazawa - p-q power theory	1983		x			x
Ferrero, Superti- Furga - Park's power theory	1991		x			x
Willems - summary of the power theories by Akagi and Ferrero	1992		x	x		x
Depenbrock -FDB(Fryze-Buchholz-Depenbrock) power theory	1993		x	x	x	x
Rosetto и Tenti - instantaneous orthogonal currents	1994		x	x		x
Nabae и Tanaka - instantaneous vector in polar coordinates	1996		x			x
Peng - Theory of generalized reactive power	1996		x			x
Peng и Lai - theory of generalized non-active power	2000	x	x	x	x	x
Power theories defined in the frequency domain						
Budeanu	1927	x			x	
Sheperd и Zakikhani	1972	x				
Czarnecki - theory of physical current components	1983 1994	x	x		Harmonic analysis	
Optimization approach						
Pasko, Siwczynski, Walczak	1985	x	x	x	x	

Table 2.2. Definitions According to the Theory of Generalized Non-Active Power [28]

Instantaneous definitions	Effective (Root Mean Square) Definitions	Average powers	Apparent Powers
$\mathbf{u}(t) = [\mathbf{u}_1(t), \mathbf{u}_2(t), \dots, \mathbf{u}_m(t)]^T$	$\mathbf{U}(t) = \sqrt{\frac{1}{T_{avg}} \int_{t-T_{avg}}^t \mathbf{u}^T(\tau) \cdot \mathbf{u}(\tau) d\tau}$		
$\mathbf{i}(t) = [\mathbf{i}_1(t), \mathbf{i}_2(t), \dots, \mathbf{i}_m(t)]^T$	$\mathbf{I}(t) = \sqrt{\frac{1}{T_{avg}} \int_{t-T_{avg}}^t \mathbf{i}^T(\tau) \cdot \mathbf{i}(\tau) d\tau}$		
$\mathbf{i}_a(t) = \frac{\mathbf{P}(t)}{\mathbf{U}_{ref}^2(t)}$	$\mathbf{i}_a(t) = \sqrt{\frac{1}{T_{avg}} \int_{t-T_{avg}}^t \mathbf{i}_a^T(\tau) \cdot \mathbf{i}_a(\tau) d\tau}$		
$\mathbf{i}_n(t) = \mathbf{i}(t) - \mathbf{i}_a(t)$	$\mathbf{i}_n(t) = \sqrt{\frac{1}{T_{avg}} \int_{t-T_{avg}}^t \mathbf{i}_n^T(\tau) \cdot \mathbf{i}_n(\tau) d\tau}$		
$s(t) = \mathbf{u}^T \mathbf{i} = \sum_{k=1}^m \mathbf{u}_k(t) \mathbf{i}_k(t)$		$\mathbf{P}(t) = \frac{1}{T_{avg}} \int_{t-T_{avg}}^t s(\tau) d\tau$	
$\mathbf{p}_a(t) = \mathbf{u}^T(t) \mathbf{i}_a(t) = \sum_{k=1}^m \mathbf{u}_k(t) \mathbf{i}_{ak}(t)$		$\mathbf{P}_a(t) = \frac{1}{T_{avg}} \int_{t-T_{avg}}^t \mathbf{p}_a(\tau) d\tau$	
$\mathbf{p}_n(t) = \mathbf{u}^T(t) \mathbf{i}_n(t) = \sum_{k=1}^m \mathbf{u}_k(t) \mathbf{i}_{nk}(t)$		$\mathbf{P}_n(t) = \frac{1}{T_{avg}} \int_{t-T_{avg}}^t \mathbf{p}_n(\tau) d\tau$	
			$\mathbf{S}(t) = \mathbf{U}(t) \mathbf{I}(t)$
			$\mathbf{P}_{app}(t) = \mathbf{U}(t) \mathbf{I}_n(t)$
			$\mathbf{Q}(t) = \mathbf{U}(t) \mathbf{I}_n(t)$

Table 2.3 presents a summary of the quantities discussed above, characterizing nonlinear and asymmetric (unbalanced) systems.

Table 2.3. Quantities in asymmetric and nonsinusoidal regimes			
Quantity, Characteristic	Designation and dimension	Fundamental powers	Non-fundamental powers
Apparent Power	$S_e(t)[VA]$	$S_{ef}(t)[VA]$ $S_f^+(t)[VA]$ $S_{He6.f}(t)[VA]$ $S_{UHe6.f}(t)[VA]$ $S_{IHe6.f}(t)[VA]$ $S_{UIHe6.f}(t)[VA]$	$S_{eN}(t)[VA]$ $S_{eH}(t)[VA]$
Active Power	$P(t)[W]$	$P_f^+(t)[W]$	$P_H(t)[W]$
Reactive Power	$N(t)[var]$	$Q_f^+(t)[var]$	$D_{eI}(t)[var]$ $D_{eU}(t)[var]$ $D_{eH}(t)[var]$
Power Factor	$PF(t)[-]$	$PF_f^+[-]$	-
Harmonic Pollution	-	-	$\frac{S_{eN}(t)}{S_{ef}(t)}$
Load Imbalance	-	$\frac{S_{He6.f}(t)}{S_f^+(t)}$	-

- **Summary critical analysis of the theoretical framework:**

The analysis of the effective values of the voltages (U_e, U_{e1} и U_{eH} $\phi - \mu$ 1.33) equation 1.33) shows that the calculated values based on these formulas are reduced. At the same time, the effective values of the currents I_e, I_{e1} и I_{eH} are increased, because the expressions for their calculation (equation 1.34) include the effective values of the currents in the neutral.

It is clear that the calculated powers, which depend on the currents, will have higher values, while those depending on the voltage values will have lower values. In accordance with the above, the second sources [87, 88, 93] recommend that the effective value of the apparent power be calculated without including the current in the neutral conductor in the effective value of the total current.

2.1 Energetic approach for assessing the deformation and imbalance of currents and voltages in the power supply system, related to power compensation.

The power theories presented in Table 2.1 by Fryze, Akagi, Peng, Budeanu, and others provide a more accurate assessment of various energy characteristics and

allow for a more complete and precise linking of the processes of Compensation of the reactive loads(RPC) with the indicators for the quality of electrical energy (QEE) in nonlinear and unbalanced regimes. This approach is necessary when developing methodological guidelines for implementing conventional RPC, but most importantly when applying modern methods for high-tech compensation using FACTS, Smart Grid, passive and active filters, and others.

In recent studies [77, 78, 123], adapted generalized indicators for assessing the quality of power systems (QPS) have been developed. The methodology is a combination of theoretical approaches and practically applicable setups. It provides the ability to analyze data sets recorded by network analyzers. By using a software application in the MathCAD environment, with matrix computation tools, it is possible to perform an express analysis of newly defined quantities.

The methodology is developed in the following sequence. Analogous to expressions (2.15), (2.16), (2.18) и (2.19) the equivalents of many (rms) voltage and current U_e and I_e are determined by the line voltages U_{12}, U_{23} и U_{31} and the line currents I_{12}, I_{23} и I_{31} :

$$U_e = \sqrt{\frac{U_{12}^2 + U_{23}^2 + U_{31}^2}{3}} ; \quad I_e = \sqrt{\frac{I_{12}^2 + I_{23}^2 + I_{31}^2}{3}} \quad (2.45)$$

The development of expressions (2.14) and (2.16) has allowed the authors [91, 95, 97] to propose practically applicable expressions for determining the rms of the fundamental voltage harmonics $U_{12f}, U_{23f}, U_{31f}$, and through the fundamental harmonics of the currents $I_{12f}, I_{23f}, I_{31f}$.

$$U_{12f} = \frac{U_{12}}{\sqrt{\frac{THDU_{12}}{100} + 1}} ; U_{23f} = \frac{U_{23}}{\sqrt{\frac{THDU_{23}}{100} + 1}} ; U_{31f} = \frac{U_{31}}{\sqrt{\frac{THDU_{31}}{100} + 1}}$$

$$I_{12f} = \frac{I_{12}}{\sqrt{\frac{THDI_{12}}{100} + 1}} ; I_{23f} = \frac{I_{23}}{\sqrt{\frac{THDI_{23}}{100} + 1}} ; I_{31f} = \frac{I_{31}}{\sqrt{\frac{THDI_{31}}{100} + 1}} \quad (2.46)$$

According to IEEE 555, TDD (Total Demand Distortion) has been introduced for voltages and currents, namely VTDD and ITDD.

$$VTDD_{12} = \sqrt{\frac{U_{12}^2 - U_{12f}^2}{U_{12}^2}} ; VTDD_{23} = \sqrt{\frac{U_{23}^2 - U_{23f}^2}{U_{23}^2}} ; VTDD_{31} = \sqrt{\frac{U_{31}^2 - U_{31f}^2}{U_{31}^2}}$$

$$\text{ITDD}_{12} = \sqrt{\frac{I_{12}^2 - I_{12f}^2}{I_{12}^2}} ; \text{ITDD}_{23} = \sqrt{\frac{I_{23}^2 - I_{23f}^2}{I_{23}^2}} ; \text{ITDD}_{31} = \sqrt{\frac{I_{31}^2 - I_{31f}^2}{I_{31}^2}} \quad (2.47)$$

The generalized three-phase coefficients VTDD_{3P} and ITDD_{3P} are determined in accordance with the following expressions:

$$\text{VTDD}_{3P} = \frac{1}{\sqrt{3}} \cdot \sqrt{\sum_{i=1}^3 \text{THD}_{U_i}^2 \cdot \frac{U_{fi}^2}{U_{ei}^2}} ; \text{ITDD}_{3P} = \frac{1}{\sqrt{3}} \cdot \sqrt{\sum_{i=1}^3 \text{THD}_{I_i}^2 \cdot \frac{I_{fi}^2}{I_{ei}^2}} \quad (2.48)$$

MAIN CONCLUSIONS AND RESULTS OF CHAPTER TWO

1. *Theoretical statements for the analysis of non-symmetric and non-linear regimes abstracted from the two main approaches – Fourier harmonic analysis and Fertescue's method of symmetric components are presented. A comparative analysis of different power theories is made depending on the basic power (average, effective or instantaneous), and also depending on the fundamental and non-fundamental powers used. The consideration is relevant to the overall concept for the analysis of nonlinear and unbalanced systems and clarifies the nature of inactive powers (deformational, pulsating, latent).*

2. *In a formalized synthesized form, the main expressions giving the relative relationship of the CRL with the quality of EE are presented. On this basis, a dualistic approach has been applied to assess the CRL, taking into account the influence of the voltage regime. The influence of the voltage deviation on the compensating power Q_k has been quantitatively determined. In a similar way, an energy approach has been applied to assess the deformation and unbalance of the currents and voltages in the ESS related to the CRL. The energy impact of the load on the PCEE, respectively on the reactive powers, has been shown. Such an approach is significantly more precise, adequate and identical and creates prerequisites for the implementation of optimal and effective CRL.*

3. *Object-oriented, practical-applied formulations for the analysis and application of CRL are presented. The application of longitudinal CRL, the features of energy processes in arc furnaces, rolling mills, welding units, industrial electronic converters and consumers introducing significant disturbances into the ESS are analyzed. Methodological guidelines for calculating and synthesizing circuit-technical formulations when applying passive and active filter-compensating devices are developed. The presented formulations aim to characterize and clarify the application of more complex and non-specific approaches to CRL in the existing wide variety of consumers in the ESS.*

CHAPTER THREE

RESEARCH ON REACTIVE LOAD COMPENSATION UNDER NONLINEAR AND ASYMMETRIC LOADING IN REAL OBJECTS

3.1 Methodology for studying the compensation of reactive loads according to the criterion "Electricity efficiency".

The most effective way to achieve electrical energy efficiency in the ESS is by reducing power and electricity losses.

Active power losses can be determined using the following methodology. In principle, it is known that the total active power losses ΔP are related to $\cos\varphi$ by the ratio:

$$\Delta P = \frac{1}{\cos^2 \varphi} \quad (3.1)$$

A. In a fully symmetrical and sinusoidal mode in the ECS.

In this case, which is not typical for the used ESS, the following expressions can be written:

$$\Delta P_a = \frac{P^2}{U^2} \cdot R \quad ; \quad \Delta P_p = \frac{P^2 + Q^2}{U^2} \cdot R = \frac{P^2 (1 + \operatorname{tg}^2 \varphi)}{U^2} \cdot R \quad (3.2)$$

where: ΔP_a – active power losses only from active load P [kW]; ΔP_p – active power losses caused by P and the reactive load $Q = P \cdot \operatorname{tg} \varphi$ (Fig. 3.1)

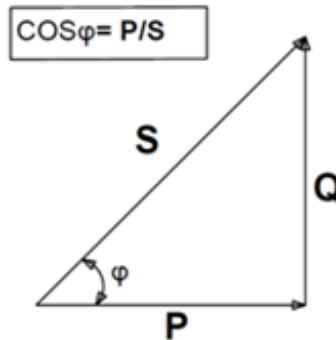


Fig.3.1.

The presence of reactive power leads to additional active losses, which can be determined by the coefficient of additional losses K_{Δ} , determined by the expression:

$$K_{\Delta} = \frac{\Delta P_p + \Delta P_a}{\Delta P_p} \cdot 100 = \operatorname{tg}^2 \varphi \cdot 100 [\%] \quad (3.3)$$

If for example, the average daily $\cos\varphi = 0,87$ i.e. $\operatorname{tg}\varphi_{cp} = 0,57$, then the reactive power Q increases by $K_{\Delta} = 0,572 \cdot 100 \% = 32,5 \%$ the total active power losses for the system.

B. In non-symmetrical and non-linear mode in the ESS.

Such an operation mode was analyzed in the second chapter – expressions (2.29÷2.39). The calculation methodology is as follows. The power factor PF is determined by the expressions [76,69]:

$$PF = \frac{P}{S_{ND}} = \frac{P}{\sqrt{P^2 + Q^2 + N^2 + D^2 + (3n+1)S_0}} = \cos \sqrt{\frac{1 - K_I^2}{1 + \varepsilon_U^2 + (3n+1)\alpha_U^2}} \quad (3.4)$$

3.2 Characteristics of the site, features of the research process and results of the study.

The studied industrial facility produces starter batteries (CB). The enterprise is characterized by uninterrupted production process, and the work cycle is three shifts. From the point of view of reliability of power supply, the facility is classified as category II, as power supply interruption is associated with a significant reduction in production, downtime of many people, mechanisms and machines. The electrical scheme of the plant is designed so that in the event of a failure of the main power supply, switching to a backup source is carried out manually.

From the regional substation (substation) "Dobrich" 110/24 kV (2 pcs. CT 2x25 MVA), via a CAXEKT 3x1x185 mm² cable with a length of about 1.2 km, electricity is supplied to a newly built GRU 20 kV, located in the existing transformer room..

The main distribution substation is a complete switchgear, SF6 version (SF6) of the ABB, GAE 630 series, 24 kV and consists of 9 sections (Fig. 3.3).

The rectifier stations, which are the most powerful consumers in the plant, are powered by three dry power transformers (CT) of 1250 kVA TP1, located in cells adjacent to the GRU room. Another group of rectifiers is powered by CT 1600 kVA, located on the periphery of the plant.

The company's power supply system has many electrical panels, which supply power to various equipment, such as WIRTZ, CON-CAST machines, MAC-15; WIRTZ-13-200; MOOJIN-30MV15; COS-machines of the BATEK, MOOJIN and TBS type; "DAGA" type machines, compressed air installations, natural gas installations, softened water installations, aspiration systems, etc. The total consumed electricity W [MWh] for the first nine months of 2019 amounted to 7796.955 MWh, with the dynamics of electricity consumption shown in Fig. 3.4.

АВР (1-2)
спершичний и
електро-маш. бломи
на опинення на промислових

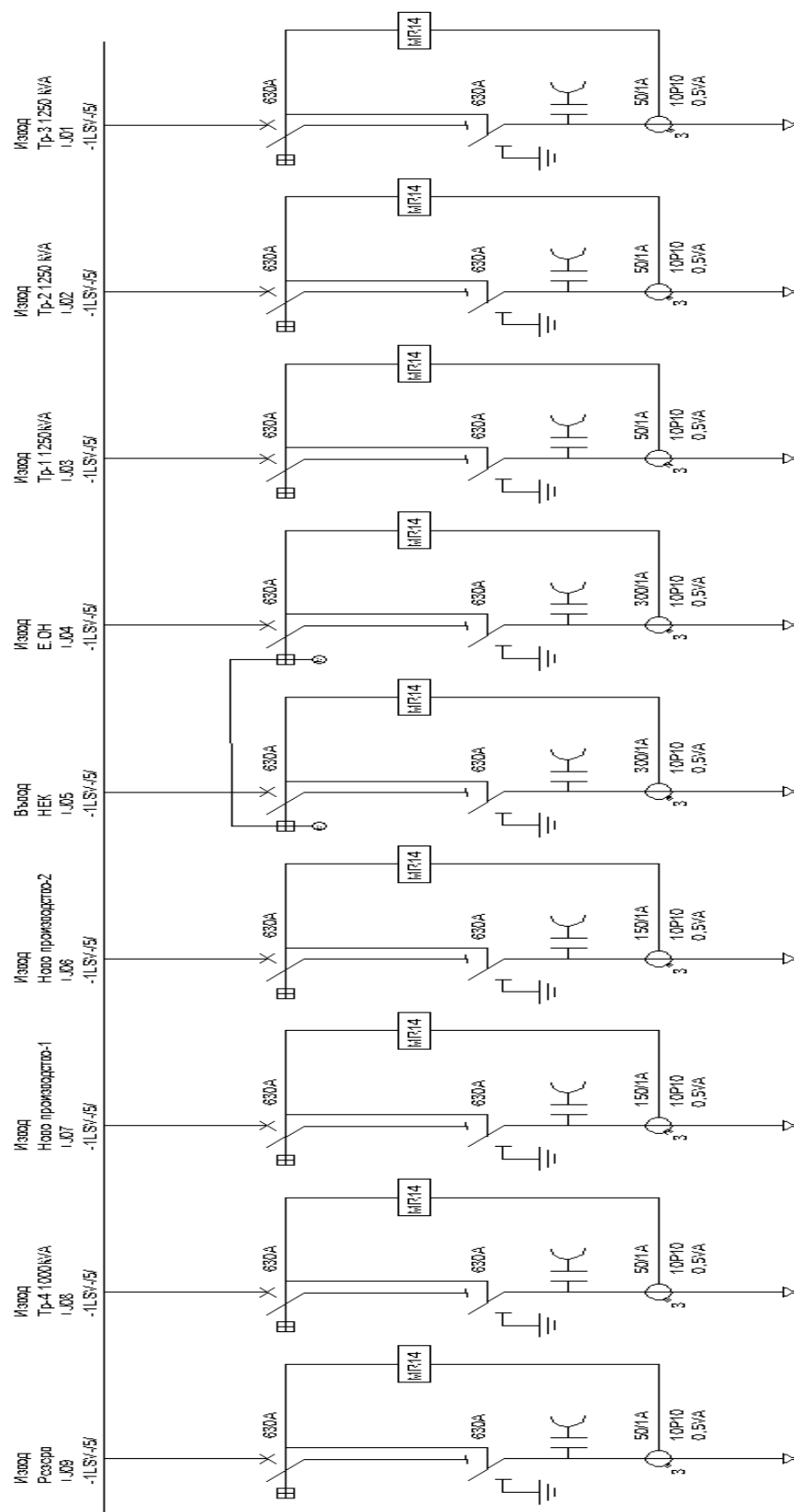


Fig. 3.3 Single-line diagram of the company's GRT

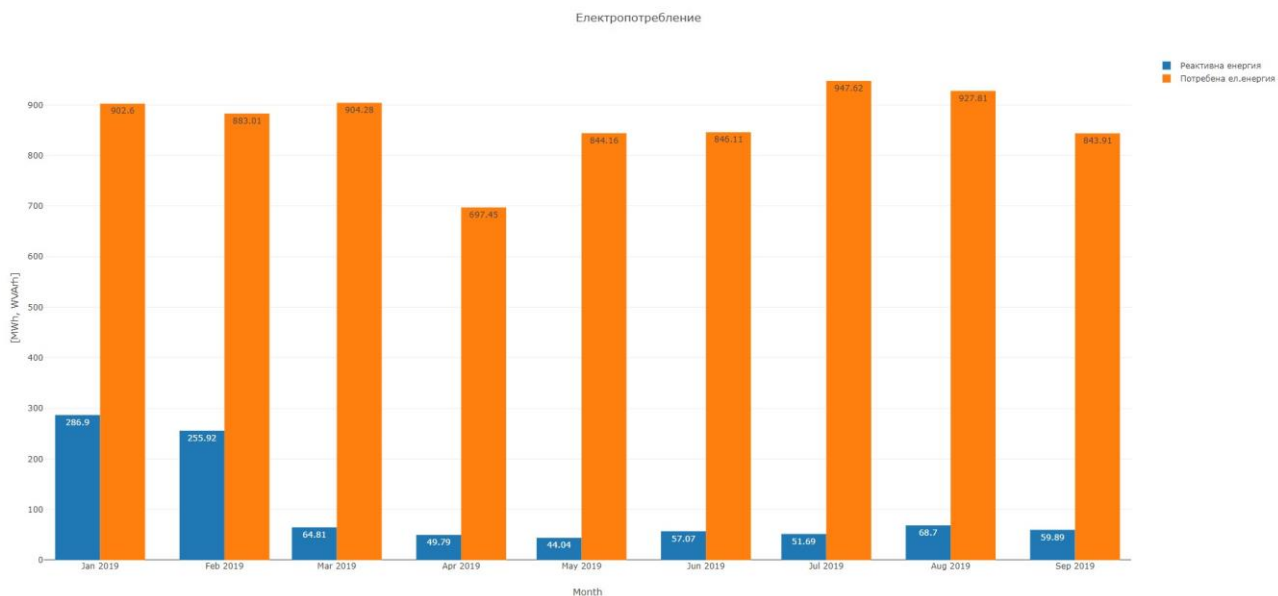


Fig.3.4 Dynamics of electromobility

The measurements were performed with a specialized transmission measurement system ISKRA Portable Network Analyzer PNA 760. By connecting a specialized device at appropriate control points, which are convenient places for connecting current sensors (normalizing converters) to the LV busbars of the two studied objects. The current sensors are openable and after opening, they cover the respective busbar, thus converting the signal that is fed to the measuring device in a scanned form. The following energy characteristics are determined:

- *At a certain sampling rate set by the instrument, the effective, average and maximum values of the phase currents and voltages are determined dynamically $I_a, I_b, I_c, U_a, U_b, U_c$.*
- *Through developed specialized software, using the data from the instrument, the active, reactive and apparent powers are determined - P [kW], Q [kVar], S [kVA], as well as the additional substances of the power - pulsating power N , associated with the asymmetric modes; "hidden" power S_0 , associated with the imbalance of the system and the deformation power D , caused by the nonlinearity of the system.*
- *The characteristics related to the quality of electrical energy are determined – voltage deviation and fluctuation $\delta U_u, \nabla U_u$ current and voltage asymmetry, estimated by the asymmetry coefficients ϵI and ϵU ; current and voltage unbalance, estimated by the coefficients αI and αU ; non-sinusoidality of current and voltage estimated by the harmonic coefficients and the integral coefficient of non-sinusoidality $K_{vI}, K_{vU}, THD_I, THD_U$.*

Based on the specificity and characteristic features of the site, as well as taking into account the previously prepared events and the established organization for research and analysis, the following objectives of the research process can be formulated:

- *To conduct objective measurements of the electrical parameters at the marked control points using a professional analyzer PNA 760, thermal camera type HT-02, infrared thermometer UT300C, goniophotometer INVENTFINE GPM 1600L, spectrophotometer AsenseTEK Lighting Passport ALP-01 and luxmeter Extech HD450, which will serve as the basis for subsequent analyses and proposals for rationalization of the ESS;;*
- *Based on the proposed methodology and purpose-developed software, to determine energy characteristics, enabling the assessment of power and electric energy losses and methods for CRL, respectively, the electric energy efficiency in the company's ESS;*
- *Based on the results of the study, to present technical solutions and approaches for improving the operation and rationalization of electricity consumption, aimed at achieving energy savings;*
- *To assess the effect of the proposed measures and innovative solutions by determining various technical and economic characteristics after implementation of the proposals, such as improved reliability, effect of the innovation in monetary equivalent, payback periods for the facilities, environmental impact, etc.*



Fig.3.5 Photos of the measuring equipment during measurement

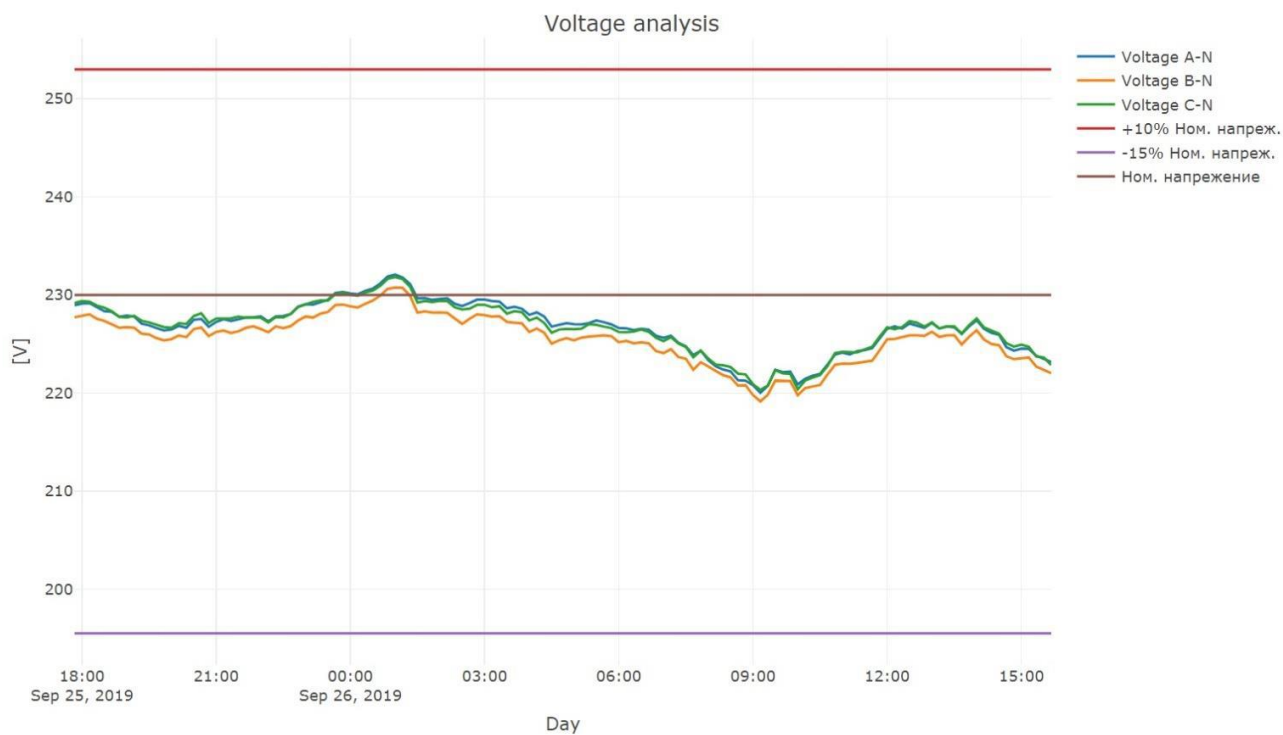


Fig.3.6. Voltage variation and compliance with limits with BDS EN50160 standard.

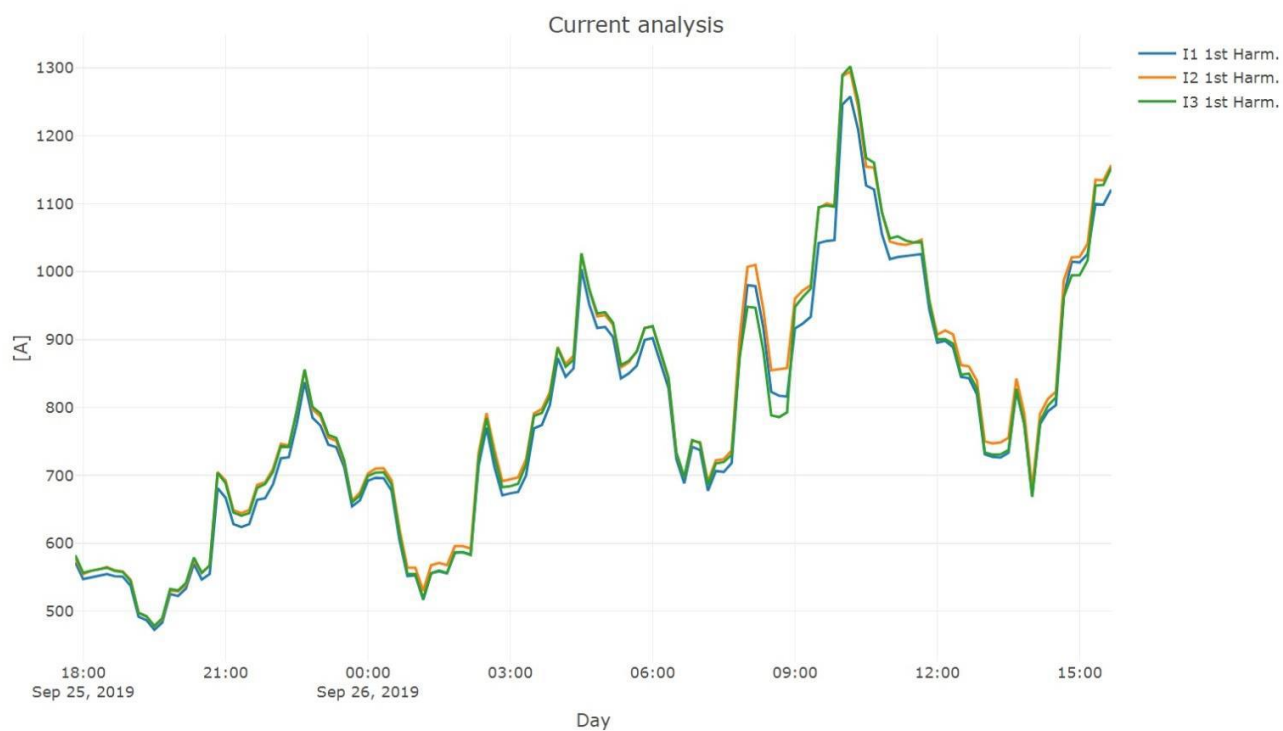


Fig.3.7. Variation of currents in phases.

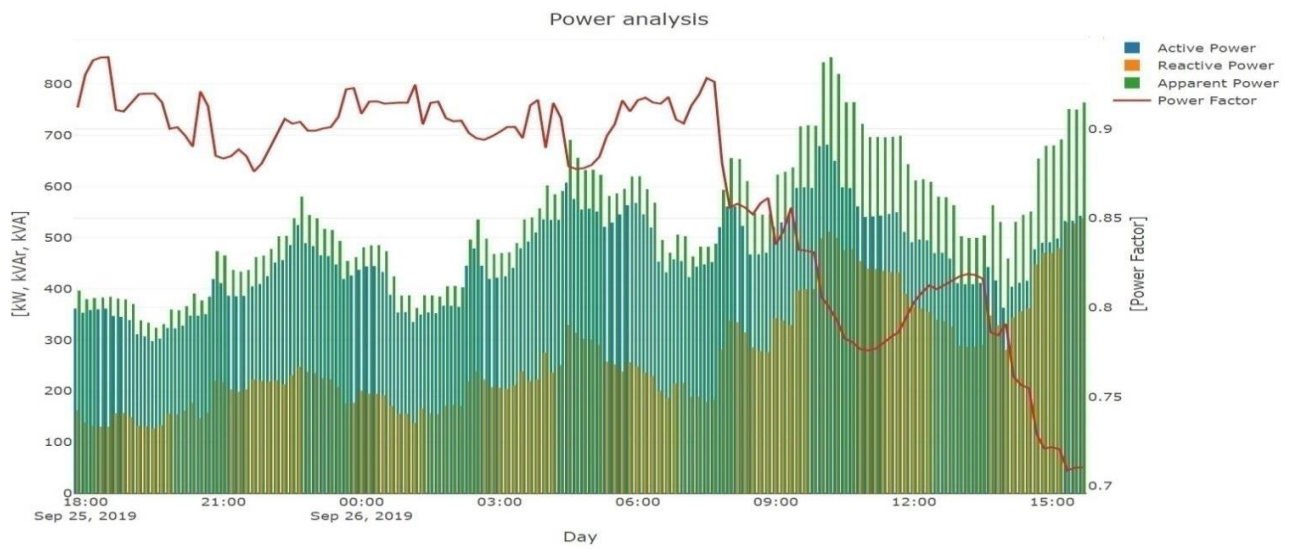


Fig.3.8. Change in active, reactive, apparent power and power factor.

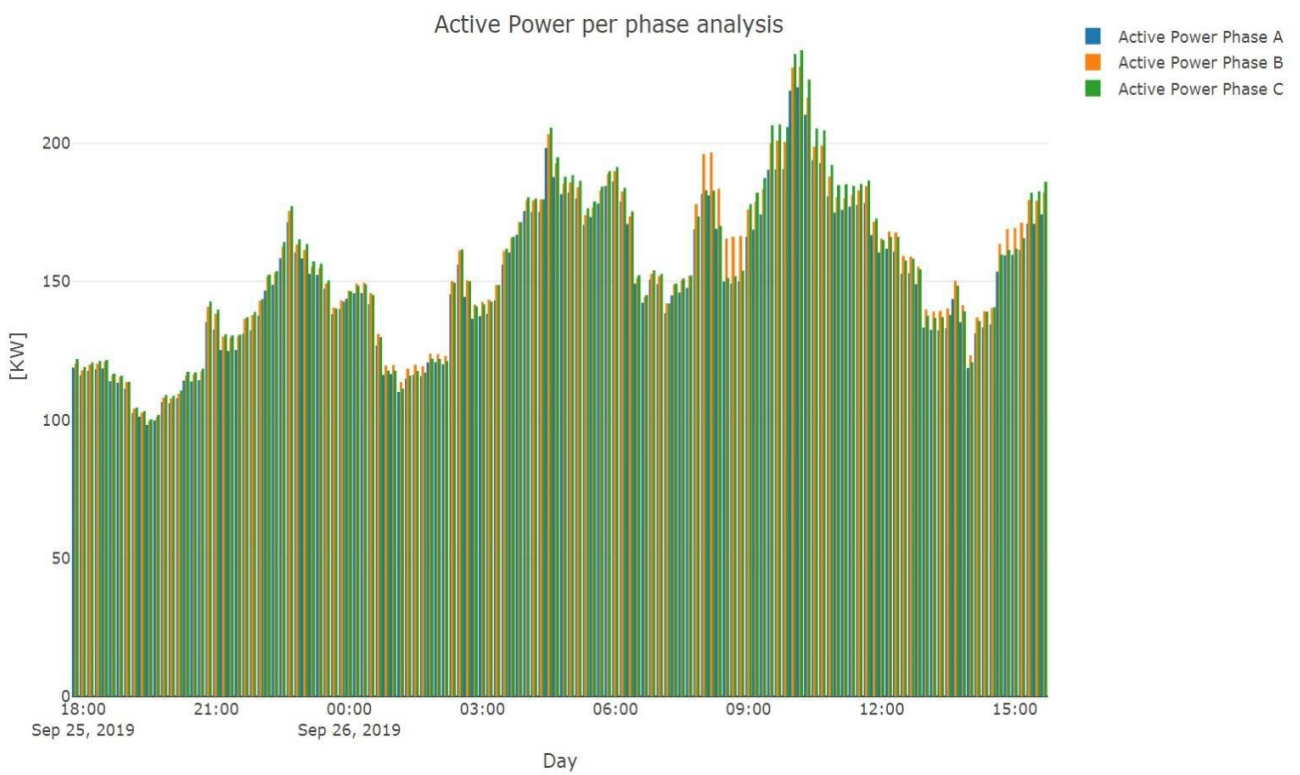


Fig.3.9. Change in active power by phases.

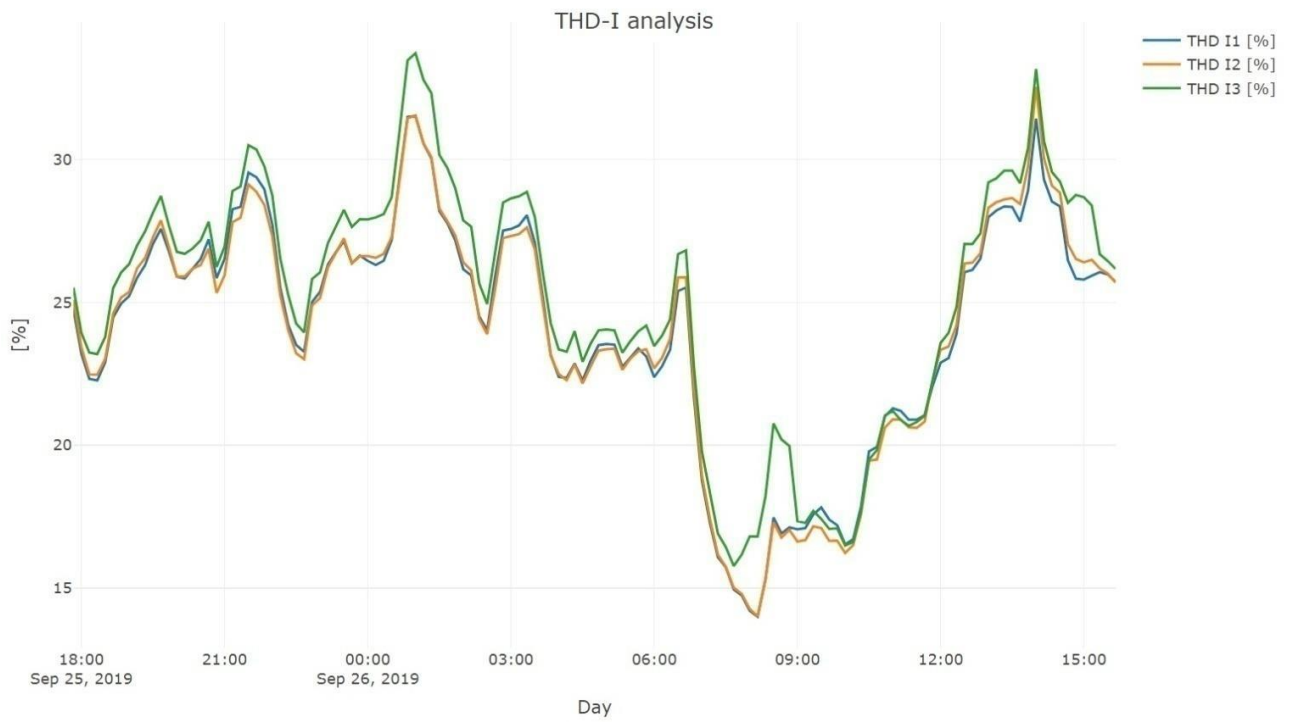


Fig.3.10. Change in the current harmonic distortion factor THD

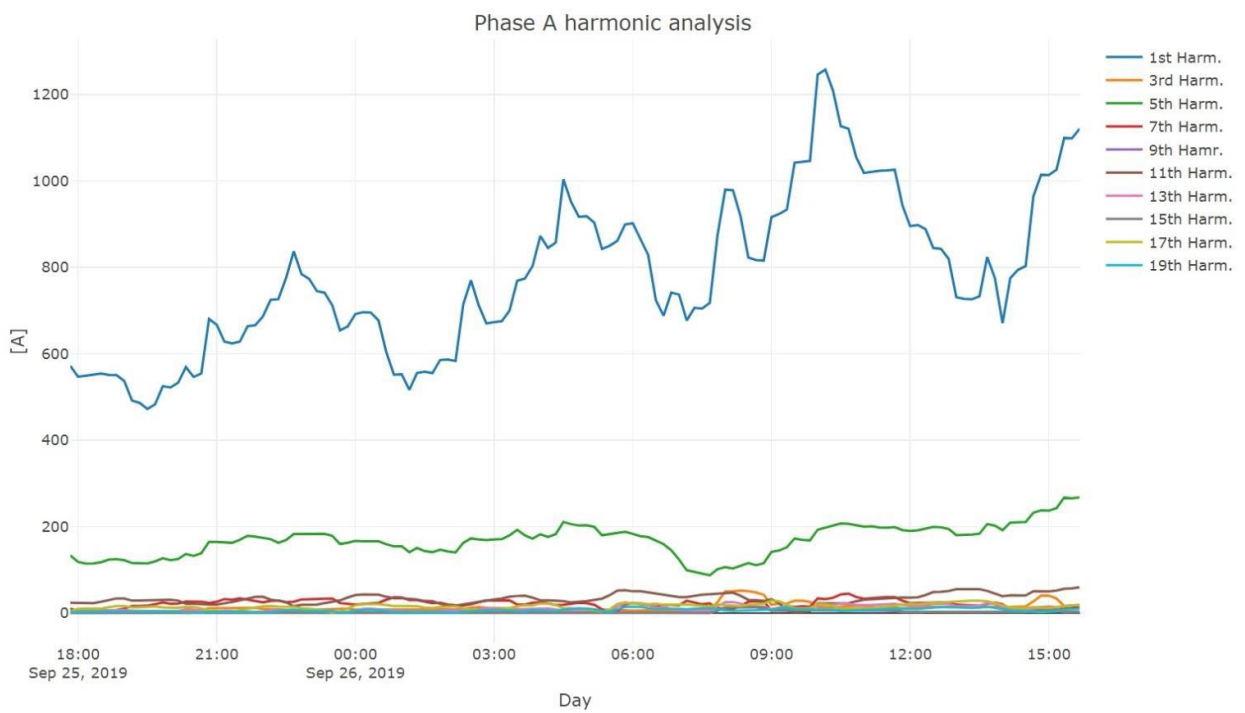


Fig.3.11. Change in the harmonic composition of the current for phase A.

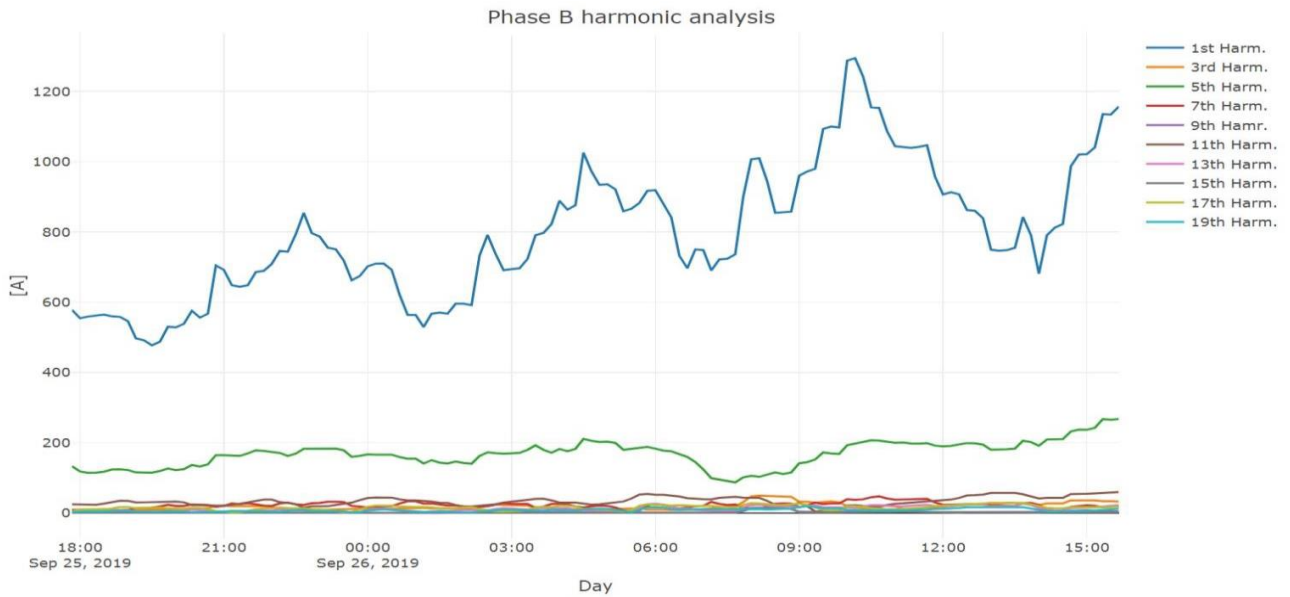


Fig.3.12. Change in the harmonic composition of the current for phase B.

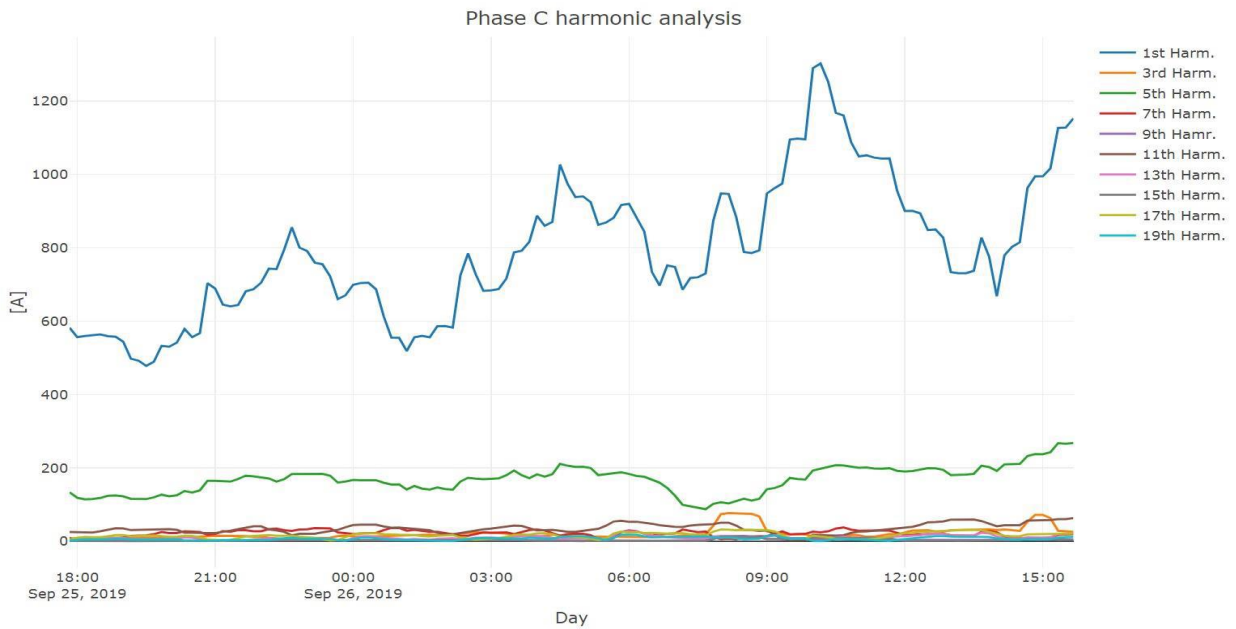


Fig.3.13. Change in the harmonic composition of the current for phase C.

Regarding the GRT of the 1600 kVA substation, the following conclusions can be drawn::

- *There is a clear dynamic in the current load, varying from 500 to 1300A.*
- *At loads from 400 to 600 kVA the power factor is in the range (0.87÷0.95) with an average value of 0.9. At higher loads in the range of 600 to 1000 kVA, the power factor drops to values (0.7÷0.85), which indicates insufficient installed power of the compensation system.*

- *The levels of higher harmonics significantly exceed the requirements of the IEC 61000 standard. THDi varies in the range (12÷40)%, with an average value of 30%. The dynamics of the change of higher harmonics follows the dynamics of the load. The mode is characterized by all the adverse effects caused by the presence of higher harmonics of the current.*

Comparative analysis of the two methods

When comparing the two diagnostic methods, troubleshooting with a thermal camera is faster and easier with exceptional accuracy and gives us an immediate diagnostic insight into the full extent of the problem. While using an infrared thermometer, we can easily miss a critical point and problem area in a given production process. To achieve the efficiency of a thermal camera with an image resolution of 60x60 pixels, we need to use 3600 infrared thermometers at the same time. But if we use a high-end thermal camera that has an image resolution of 640x480 pixels, 307200 pixels or using 307200 infrared thermometers we will reach the values of a thermal camera.

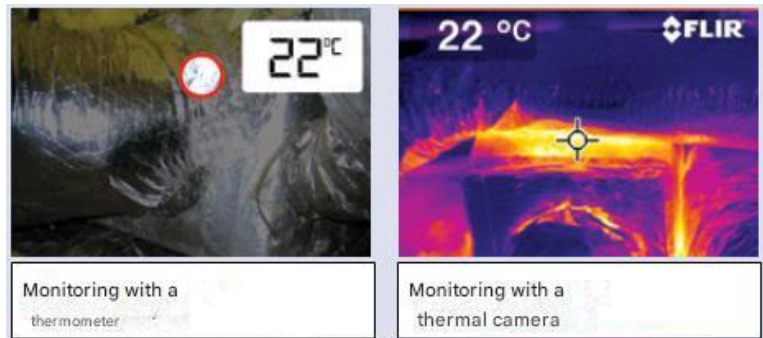


Fig 3.16. Visual comparative analysis

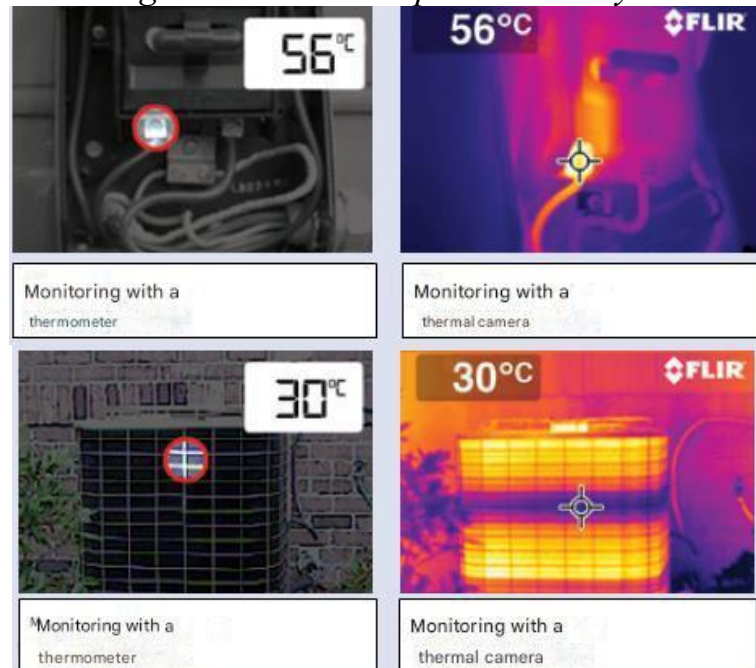


Fig.3.17. Visual comparative analysis

Research on CCU

The switchgear is installed in the rectifier room. It is divided into two sections, each protected by a CVS630F circuit breaker manufactured by Schneider Electric, and then connected to the power busbar of the PT 2-1 BB-3 panel. Two temperature measurements were carried out with an infrared thermometer and an infrared camera, with the higher values being recorded with the infrared thermometer due to the fact that the measurements were carried out in different periods and the load changed.

Fig. 3.18 – 3.20 show thermal imaging screens from measurements of switching and protective elements in the switchgear. The measured temperatures significantly exceed the standards for this type of protection. Exceeding the permissible temperatures leads to the release of additional heat, which is actually a loss of active electricity. Additional heating is also caused by incorrect calculation of the cross-section of the connected wires - with smaller cross-sections they become a source of heat, as is the case in Fig. 3.18, and with more massive ones, heat is taken from the circuit breaker and transferred along the length of the cable.

When the current increases above the nominal to $I \leq 1,3I_N$ the circuit breaker should not trip, and this causes significant heating of the circuit breaker parts. In such a mode, the majority of switching and protective devices in the switchgear operate, and the reason for the increased current is the generation of higher harmonics.



Fig.3.18

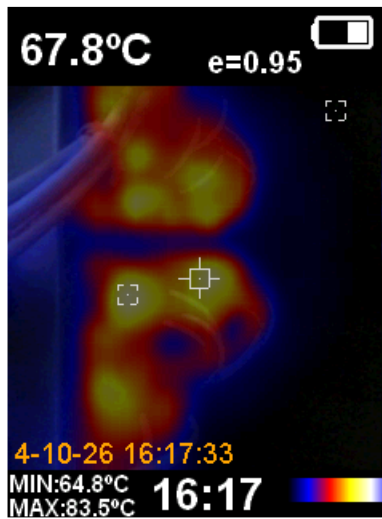


Fig.3.19



Fig.3.20

The tests conducted on CVS630F circuit breakers (Fig.3.21). Excessively high temperatures of the contact connections were recorded (Fig.3.22 – Fig.3.23), as well as high temperatures of the protection devices themselves. Carbon deposits were also observed on the base of the cable lugs, where the connection to the cable is.

The switching capacity of the circuit breaker can reach up to 150 kA and wear resistance up to 3000 switching cycles. The circuit breaker protects against overloads and has a thermal memory that can be used for thermal mode analysis.



Fig.3.21



Fig.3.22



Fig.3.23

Fig. 3.24 presents the next element of the KKV that was studied, namely the capacitor banks themselves and their power cables. Fig. 3.24 clearly shows the thermal sticker that indicates the nominal (maximum permissible) temperature of the battery (temperature range $-40 +60^{\circ}\text{C}$). The measurement carried out with a thermal camera (Fig. 3.25) and an infrared thermometer shows that it does not correspond to the actual temperature, which significantly exceeds it (about 84°C). Also, the temperature of the power cables is too high for such a facility - over 50°C (Fig. 3.26). The probable reason for this, confirmed by previous studies, is a high level of higher harmonics of the current in the system and poor cooling.

The capacitor banks studied in the KKV are of the propylene type. In principle, it is considered that these batteries operate "cold", i.e. with average daily temperatures of less than 20°C with much lower dielectric losses compared to oil-filled ones (less than 0.003kW/kVAr). In addition, such types of batteries have a reduced sensitivity to higher harmonics of the current, i.e. the active losses from higher harmonics that are deposited in them should be insignificant. In practice, in this particular case, this is not the case, moreover, it was found that some of the batteries are defective.



Fig.3.24

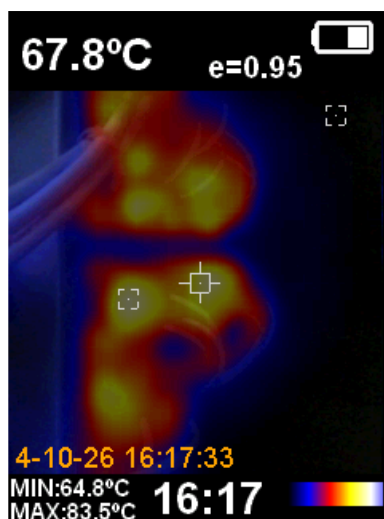


Fig.3.25



Fig.3.26

Study of the defect coefficient

Table 3.2 and Table 3.3 present the results of the calculations for the defect coefficients of the output cable of the KКУ, the input cable of the Compressor panel, the main switch of the Charging system 2C-RC-220V/150A, the power transformer of the CR800/360V. All calculated values for K_D are in the range:

$$1,2 \leq K_D \leq 1,5$$

Such a condition of the investigated facilities is characteristic of the occurrence of a process with an increased probability of failure and it is necessary to take adequate measures to improve their condition before the emergency situation occurs.

Table 4. K_D values for the output cable of the KКУ and the input cable of the Compressor panel

	Output cable of the KКУ (thermometer)			Incoming cable to panel Compressor		
Phases	A	B	C	A	B	C
$\Delta T_{KC} [^{\circ}C]$	11,3	11,9	12,4	16,5	17,4	18,9
$\Delta T_{np} [^{\circ}C]$	9,65	9,22	9,46	12,5	12,7	13,3
K_D	1,17	1,29	1,31	1,32	1,38	1,42

Table 5. K_D values for the main circuit breaker of the Charging system 2C-RC-220V/150A and the power transformer of the CR800/360V

	Charging system main switch 2C-RC-220V/150A			Power transformer of CR800/360V		
Phases	A	B	C	A	B	C
$\Delta T_{KC} [^{\circ}C]$	18,3	18,9	18,1	15,7	16,1	15,9
$\Delta T_{np} [^{\circ}C]$	12,8	12,8	12,8	12,8	12,6	12,7
K_D	1,43	1,47	1,41	1,23	1,28	1,25

MAIN CONCLUSIONS AND RESULTS OF CHAPTER THREE

- 1. In modern industrial facilities, the majority of consumers have a nonlinear and asymmetric nature, significantly worsen the quality indicators of EE and require a special approach to the processes of CRL. In this regard, based on existing developments, a methodology for the research process in CRL according to the criteria "Electric energy efficiency" is proposed. The statement confirms and analyzes not only the classical active and reactive powers, but also the emergence, behavior and consequences of additional substances of power - pulsating, latent and deformation power. For their study, it is necessary to create adequate and computational procedures, and in the research process to use multifunctional technical means, possessing high accuracy and precision. The methodology has a clearly expressed practical-applied nature and universal application for facilities from different industries and with different energy characteristics.*
- 2. The presented methodology was tested in a large industrial facility, saturated with nonlinear and unbalanced consumers. Using a specialized network analyzer, various energy indicators and characteristics were measured and analyzed for 35 days in two operating modes - at reduced and normal load. A strong asymmetry and non-sinusoidality of the electrical quantities were found, and these indicators were more pronounced in the reduced load mode. The analysis gives reason to assume that there is equivalence for the application of technical means for CRL in both operating modes, i.e. it is also necessary when operating the facilities in the minimum load mode.*
- 3. The partial losses of active power from pulsating, latent and deformation power are determined in a differentiated form. The sum of all losses from the input PCEE is comparable to the active conventional power losses, which is a negative finding. The power factor has low values and varies within the limits $PF=(0.713\div0.751)$. This shows that the personal CRL system works extremely inefficiently and it is imperative to completely change the CRL concept and apply fundamentally new adequate approaches, consistent with the principles of the proposed methodology.*
- 4. To confirm the negative findings of the research process, diagnostic tests were conducted using infrared thermography with two technical means - infrared thermometers and an infrared thermal camera. Various elements of the compensating systems were examined and defective KB and an increased probability of defecting the remaining elements of the KKV were found - the defectivity coefficient varies within the limits of $1.2 \leq Kd \leq 1.5$. In this regard, measures have been proposed to rationalize the CRL by applying anti-resonance protection, controlling the compensation system by a reactive power regulator operating on the criteria of "direction and magnitude of reactive power", implementing sequential active filters and implanting SCADA and other high-*

tech means for monitors, control and management. This will lead to savings in electricity within (3÷4)% of the total consumption with a payback period of the facilities (3÷5) years.

- 5. For the studied objects, an assessment was made of the three-phase, power-weighted indicators developed in section 2.3 in connection with the CPT. A comparative analysis of these indicators with the conventional ones was made and it was found that they have lower values than the traditional standardized indicators. Therefore, the load reduces these indicators and the CPT process must take this fact into account. In this regard, taking into account the strongly pronounced asymmetric and non-sinusoidal mode of electricity consumption in the studied object, it is proposed to determine the necessary compensating power Q_k using the power factor PF , and not $\cos\varphi$. The determination of PF can be done both on the basis of the methodological guidelines developed in section 3.1 and using the power-weighted indicators. In this regard, a formulation is presented for precise calculation of the overload of filter-compensating systems.*

CHAPTER FOUR

RESEARCH ON THE POSSIBILITIES OF OPTIMIZING CRL USING SD AND KB

1.1. Description of the technological process with a technological scheme of the researched object

The object of the study is a large industrial enterprise. Its activity is related to the production and sale of light and heavy soda ash. In addition to these products, soda bicarbonate, purified brine and lime are produced and sold. The main raw materials for production are limestone, brine, steam and electricity, which the company supplies through its subsidiaries.

The production of soda ash at Solvay-Sodi AD is divided into separate stages in workshops shown in Fig. 4.1:

Lime production - consists of three workshops: **“Ropeway workshop”**, **“Peshten”** and **“Gasilen”**.

The **“Ropeway workshop”** is 7.2 km away from the plant. It has a capacity of 1.6 million tons of limestone per year, or 270 tons per hour. The Ropeway includes the small ropeway above the limestone bunkers of the lime kilns; the warehouse; the coke crushing and sorting department; the system of conveyor belts for coke and limestone from the warehouses to the lime kiln bunkers..

The **“Peshten”** workshop is the second in the technological order of lime production. The main facility of the workshop is the lime kilns. They are the largest and heaviest facilities in the entire plant. Each kiln has a capacity of 300 tons of lime per day. The **“Gasilen”** workshop is not large, it produces milk of lime, which is an aqueous suspension of calcium hydroxide.

“Absorption and distillation” – the largest and most technologically complex workshop. There are three independent lines, each of which has a capacity of 400 thousand tons of soda per year. Each technological line has three distillation and three absorption elements. This workshop also includes three pumping stations – a sludge pumping section, collectors for ammoniated brine and filter liquid and an ammonia station for ammonia water and sulfide.

“Carbonation and filtration” – the main stage of the carbonation process is carried out in this workshop. Sodium bicarbonate crystals are formed and their subsequent separation from mother liquor. In technological terms, it is also formed by three technological lines. Each of them includes two series of carbonation columns and five vacuum filters.

“Calcination, heavy soda and cooling”:

“Calcination” means thermal decomposition of sodium bicarbonate. This is the final stage of the production of soda ash. 7 calciners with hydromotor drive have been installed in the workshop

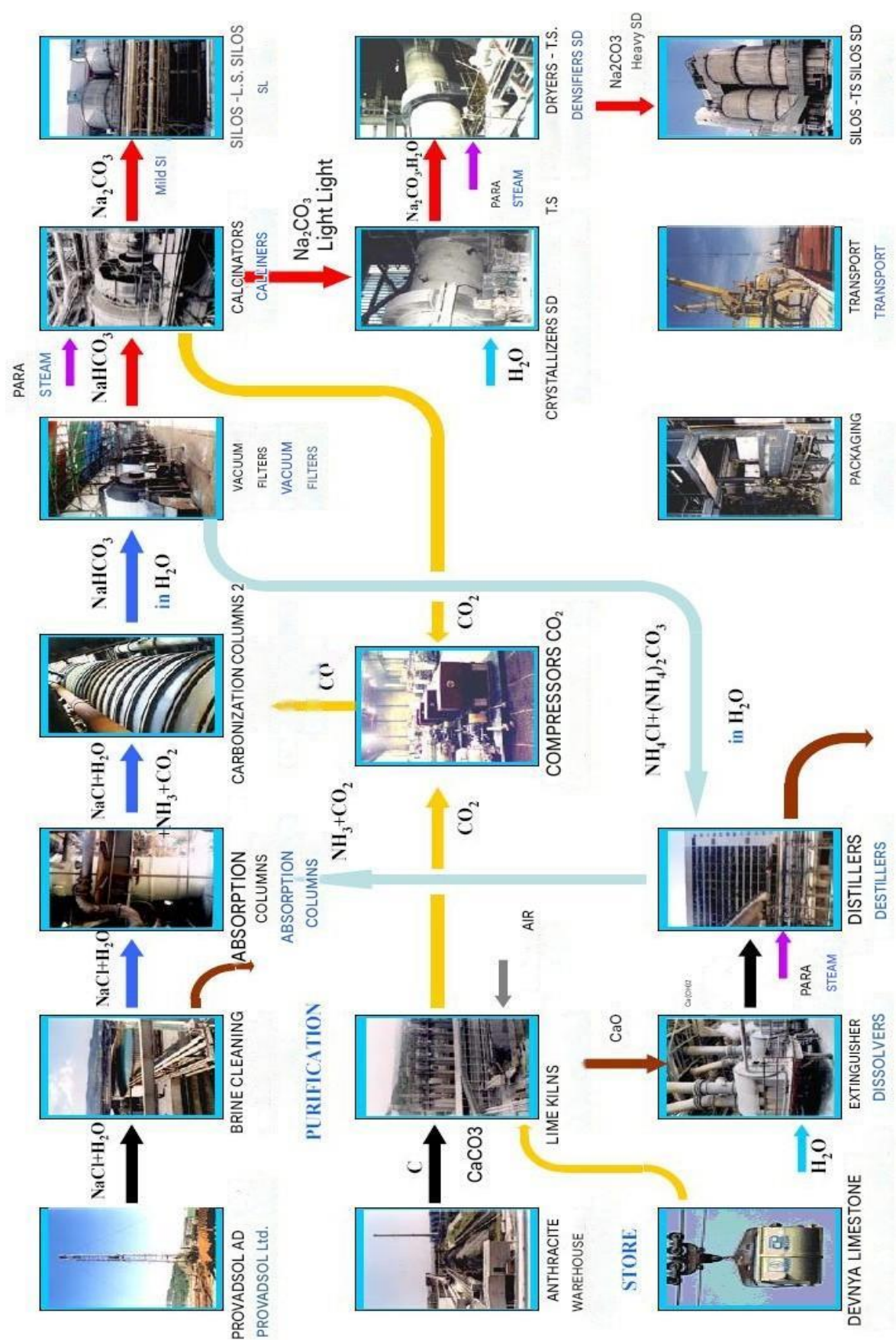


Fig. 4.1 Technological scheme of the site

In the “**Heavy Soda**” workshop, the light soda obtained in the “Calcination” is moistened with water and the so-called monohydrate is obtained. After drying by heating, in which the crystalline structure of the soda is preserved, heavy soda is obtained. Its bulk weight is 0.9 tons per cubic meter. Three technological lines have been built, each with a capacity of 400 thousand tons per year. Heavy soda is stored in two silos of 6 thousand tons and one for 18 thousand tons.

In the “**Cooling**” workshop, the soda reaches a temperature of 150-170 °C. But in order to be packed in bags, the temperature must be lowered to 40-60 °C. This is done by rotating cooling drums with a capacity of 50 tons per hour. The cooled soda is stored in six silos with a capacity of 6 thousand tons each.

“**Packaging and Shipping**” from this workshop, soda ash is shipped in several ways:

- *in loose bags;;*
 - *loose bags on pallets wrapped with shrink wrap;*
 - *loose bags in self-supporting packages with shrink wrap;*
 - *in bulk in plastic containers /soft containers/;*
 - *in bulk in road and rail tankers;*
 - *in bulk in 20-foot metal containers /GTK/;*
- in bulk for ships via regional transport system /RT/;*

1.2. Analysis of the site's ESC

The main power supply of the site is provided by the Deven Thermal Power Plant. At present, the Siemens SCADA POWER CC dispatching system has been introduced at the Deven Thermal Power Plant. The system manages and controls the operation of the entire power supply system on the territory of the Deven Thermal Power Plant and the site, including generators, power transformers and operational switching.

The voltage level in the thermal power plant is maintained within 21.78÷22 kV with a frequency of 50 Hz. The power factor $\cos\varphi$ is maintained within 0.85÷0.90 automatically or manually. At this stage, the excitation of the synchronous generators is carried out manually, since the automatic excitation regulators are slow-acting.

The power system is implemented with two 21/6.3 kV GPPs (No. 2 and No. 3), one GRP (No. 1) and twenty-five CPs. The connection of GPP No. 2, No. 3 and GRP No. 1 with the “SCADA POWER CC” system is implemented with input-output modules type 6MD6130 of the “Siemens” company installed in each substation. They monitor the control and perform the switching on and off of all transformer terminals. The control of the motor terminals is carried out from the workshop halls. A single-line diagram of the industrial enterprise is shown in Fig. 4.2.

The power transformers of GPP No. 2 and No. 3 are supplied with a voltage of 20 kV from the third and fourth sections of GPP-TEC “Deven” through cells with SF6 circuit breakers 1250 A manufactured by “AREVA”. For protection and control of the transformer terminals, multifunctional devices of the SIPROTEC 7SJ635 and 7SJ62 type from “Siemens” are installed, which are used as:

- *directional maximum current protections;*
- *directional protections from HP to ground, overload protections;*
- *maximum current protections for reverse sequence currents;*
- *protections from undervoltage and overvoltage;*
- *overload protections;*
- *device for backup failure of the circuit breakers /UROP/;/;*
- *control the limit values of I , U , P , Q , f , $\cos\varphi$ etc.;*

The connection of the Deven TPP with the GPP No. 2 and No. 3 is made using copper cables 12/20 kV type N2XSY, 1x185 mm². The power cables to the GPP No. 3 are one per phase, and to the GPP No. 2 are two in parallel for each phase laid in a cable tunnel.

4.2.1 Main step-down substation No. 2.

MSDS No. 2 consists of two two-winding transformers (TR21S and TR22S) type TMRU 20 000/21 with on-load voltage regulation.

To reduce the area and volume of the substation, it is built on the basis of a switchgear consisting of four sections. For control and monitoring of the input and sectional cells, multifunctional protections of the “SIPROTEC” 7SJ64 type are installed.

Technical parameters of the power transformers are::

- *Connection diagram and group* *Dyn-11*
- *Cooling mode* *ONAN/ONAF*
- *Rated full power* *ONAN 16 000 kVA*
ONAF 20 000 kVA
- *Nominal frequency* *50 Hz*
- *Short circuit voltage u_k %* *12 %*
- *No-load current i_o %* *0,37 %*
- *Active power losses in the transformer steel at no-load $\Delta p_{cm} = \Delta p_0$*
14 kW
- *Active power losses in the transformer copper at rated load $\Delta p_M = \Delta p_{KC}$*
ONAN 75 kW
ONAF 116 kW

The cable connections of the transformers are made with removable plug-in connectors of the “CONNEX” type from the Austrian company “PFISTERER”.

For protection against damage in the GPP, multifunctional protections of the SIPROTEC 7UT61 type from the company “Siemens” are installed, used as: differential protection; maximum current protection of 6 kV; ground protection; thermal overload protection; and in the transformers: gas detector of the expansion vessel type FS9063-46 with one electrical contact; oil temperature indicator with the possibility of remote control and two electrical contacts; oil level indicator in the expansion vessel with two electrical contacts; oil level indicator in the expansion vessel

for the Jansen regulator with two electrical contacts; pressure safety valve with two electrical contacts; gas protection implemented with a gas relay (Bucholtz) type BR80MA (two systems); “cut-off valve” with one electrical contact (triggers a sudden oil consumption in the boiler and prevents its leakage from the expansion vessel); protective relay for the Jansen regulator type URF25/10 with one electrical contact; a temperature indicator with the possibility of remote control and three electrical contacts is installed on phase X2; current transformers type TMV-56 for a nominal current of 600/1 A, a nominal power of 15 VA, and an accuracy class of 5P20 are installed on the primary windings H1, H2 and H3; on the secondary winding X1 a current transformer type TMV-56 is installed for a rated current of 2000/1 A, a rated power of 15 VA, and an accuracy class of 5P5 (for the automatic voltage regulator); on the secondary winding X2 a current transformer type TMV-56 is installed for a rated current of 2000/1 A, a rated power of 15 VA, and an accuracy class of 5P5 (for protection in combination with the temperature indicator); on the secondary winding X3 a current transformer type TMV-56 is installed for a rated current of 1800/1 A, a rated power of 15 VA, and an accuracy class of 5P20 (for protection).

The regulation of the voltage under load on the 20 kV side is carried out by means of a Jansen regulator with a motor drive type RS12Δ400 41.5 10 09 1W, manually or automatically by means of a controller type TAPCON 260 manufactured by the company “MR”-Germany. The control controllers are connected to the “SCADA POWER CC” system. The regulation stages of the Jansen regulator are given in Table 4.1.

Table. 4.1 Janssen regulator stages for TR21S and TRS22S

Position of the regulator	Side 20 kV			Side 6 kV		
	U kV	I A		U kV	I A	
		ONAN	ONAF		ONAN	ONAF
1	22,05	419,0	523,7	6,3	1466,3	832,9
2	21,79	424,0	530,0	6,3	1466,3	832,9
3	21,53	428,2	536,4	6,3	1466,3	832,9
4	21,26	434,5	543,1	6,3	1466,3	832,9
5	21,00	439,9	549,9	6,3	1466,3	832,9
6	20,74	445,5	556,8	6,3	1466,3	832,9
7	20,48	451,2	564,0	6,3	1466,3	832,9
8	20,21	457,0	571,3	6,3	1466,3	832,9
9	19,95	463,0	578,8	6,3	1466,3	832,9

4.2.2 Main step-down substation No. 3.

MSDS No. 3 consists of two two-winding transformers (TR31S and TR32S) type TMRU 12 500/21 with on-load voltage regulation and two sections based on the switchgear.

Technical parameters:

- *Connection diagram and group* *Dyn-11*
- *Cooling mode* *ONAN/ONAF*
- *Rated full power* *ONAN 10 000 kVA*
ONAF 12 500 kVA
- *Nominal frequency* *50 Hz*
- *Short circuit voltage u_k %* *7,2 %*
- *No-load current i_o %* *0,52 %*
- *Active power losses in the transformer steel at no-load $\Delta p_{cm} = \Delta p_0$* *12 kW*
- *Active power losses in the transformer copper at rated load $\Delta p_M = \Delta p_{kc}$*
- *ONAN* *45 kW*
ONAF *69 kW*

The regulation stages of the Jansen regulator are given in Table 4.2.

Table 4.2 Janssen regulator stages of TR31S and TR32S

Regulator position	Side 20 kV			Side 6 kV		
	U kV	I A		U kV	I A	
		ONAN	ONAF		ONAN	ONAF
1	22,05	261,8	327,3	6,3	916,4	1145,5
2	21,79	265,0	331,2	6,3	916,4	1145,5
3	21,53	268,2	335,3	6,3	916,4	1145,5
4	21,26	271,5	339,4	6,3	916,4	1145,5
5	21,00	274,9	343,7	6,3	916,4	1145,5
6	20,74	278,4	348,0	6,3	916,4	1145,5
7	20,48	282,0	352,5	6,3	916,4	1145,5
8	20,21	285,6	357,1	6,3	916,4	1145,5
9	19,95	289,4	361,7	6,3	916,4	1145,5

The star centers of the secondary windings of the transformers TR31S and TR32S are grounded through active resistances of 40 [Ω]. The transformers have the possibility of parallel and separate operation, but currently they operate separately. For control and monitoring of the input, output /for GRP No. 1/ and sectional cells, multifunctional protections of the “SIPROTEC” 7SJ64 type are installed.



Fig. 4.6 Actual active power consumed by Tp-p 21S



Fig. 4.7 Actual reactive power consumed by Tp-p 21S

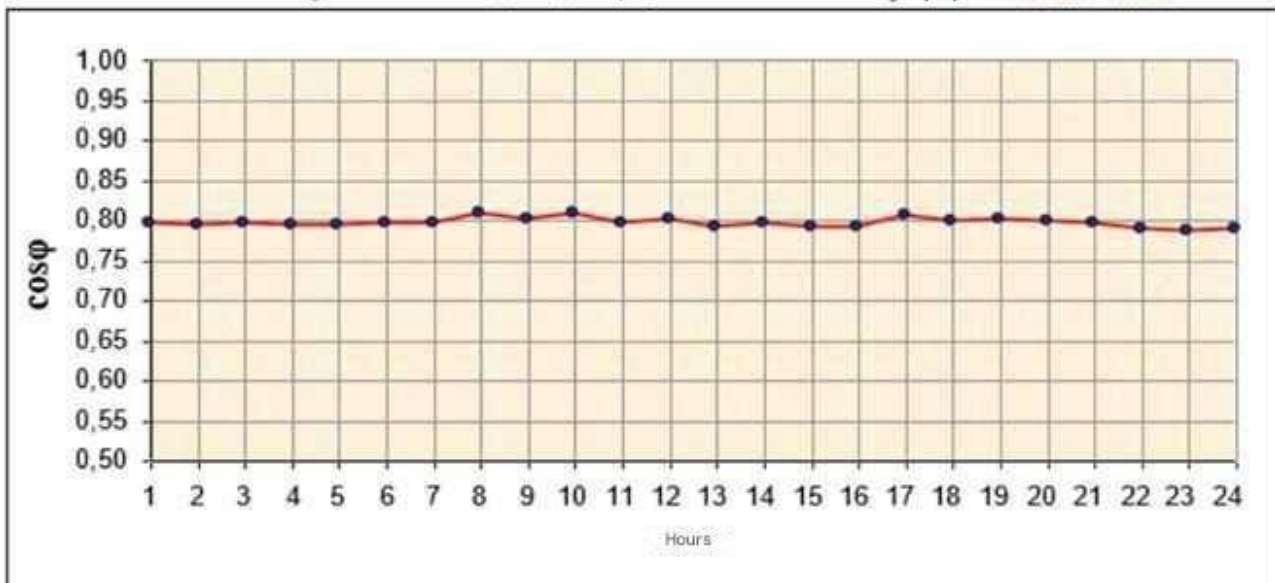


Fig. 4.8 Real $\cos\phi$ of Tp-p 21S

4.4. Analysis of synchronous motors in the EU of the studied object

4.4.1 Technical data for SM

A total of 8 synchronous motors are installed on the territory of the enterprise. Two of them are installed to be used as compensators and are powered by the first and second sections of the GPP№2, respectively, but are not currently used. The remaining 6 synchronous motors are tied to the technological process and are used to drive “High-pressure water pumps”. They are powered by the first and second sections of the GRP№3. The number of operating pumps is determined depending on the technological needs and the load of the enterprise. In principle, two pumps are used.

Technical data for synchronous motors and their excitation systems are given in Table 4.7 and Table 4.8

The exciters of the synchronous motors have the ability to control the excitation current in automatic, manual, emergency and test modes. The compensating capabilities of the installed synchronous motors are given in Table 4.7.

Table. 4.7 Technical data for SM

Technological position	SM type	P _n kW	Q _n kVar	U _n kV	I _n A	КПД η %	cosφ	PMs _s -1	q %
High pressure pump №1	СДН 15-39-10	1000	511	6	113	94,6	0,9	600	45,5
High pressure pump №2	СДН 15-39-10	1000	511	6	113	94,6	0,9	600	45,5
High pressure pump №3	СДН 15-39-10	1000	511	6	113	94,6	0,9	600	45,5
High pressure pump №4	СДН 15-39-10	1000	511	6	113	94,6	0,9	600	45,5
High pressure pump №5	СДН 15-39-10	1000	511	6	113	94,6	0,9	600	45,5
High pressure pump №6	СДН 15-39-10	1000	511	6	113	94,6	0,9	600	45,5
Synchronous compensator	ДСП-140-74-4У4	3150	1610	6	350	96,6	0,9	1500	45,5
Synchronous compensator	СДН-2-16-56-10У3	1000	511	6	113	95,1	0,9	600	45,5

Table. 4.8 Technical data for excitation system

Technological position	Excitation system	U_н вьзб. [V]	I_н на вьзб. нам. [A]
High pressure pump №1	Thyristor TBE-320/75 T-6 УХЛ4	59	320
High pressure pump №2	Thyristor TBE-320/75 T-6 УХЛ4	59	320
High pressure pump №3	Thyristor TBE-320/75 T-6 УХЛ4	59	320
High pressure pump №4	Thyristor TBE-320/75 T-6 УХЛ4	59	320
High pressure pump №5	Thyristor TBE-320/75 T-6 УХЛ4	59	320
High pressure pump №6	Thyristor TBE-320/75 T-6 УХЛ4	59	320
Synchronous compensator	Thyristor TB-630 Y4	30	500
Synchronous compensator 1MW	Thyristor TBE-320/48 T-6 УХЛ4	48	232

4.4.2 Determining active power losses of synchronous motors.

The losses ΔP_{cd} depend on the nominal active power of the synchronous motor and the speed: the lower the power $P_{н\ cд}$ and the speed, the greater the losses in the motor for generating reactive power.

For a group of parallel operating synchronous motors of the same type with the same operating mode, the magnitude of the total losses ΔP_{cd} , determined for generating reactive power Q is equal to:

$$\Delta P_{cd} = \frac{D_1}{Q_{Hcd}} \cdot Q + \frac{D_2}{Q_{Hcd} \cdot N} \cdot Q^2 \quad (4.1)$$

where: Q – total reactive power generated by a group of N motors; D_1 и D_2 – constant coefficients depending on the technical parameters of the synchronous motors. The values of the coefficients D_1 и D_2 for different types of motors are shown in Table 4.9.

Table. 4.9 The coefficients D1 and D2 for SM

Engine type	Rated power		Efficiency %	Coefficient, kW	
	P _Н , kW	Q _Н , kVAr		D ₁	D ₂
1000 rpm					
СДН-14-49-6	1000	511	95,37	5,09	3,99
СДН-14-59-6	1250	633	95,95	4,74	4,42
СДН-15-30-6	1600	812	95,75	6,65	6,8
СДН-15-49-6	2000	1010	96,06	8,06	7,53
СДН-15-64-6	2500	1260	96,5	8,13	7,74
СДН-16-76-6	3200	1610	96,75	10,3	8,91
СДН-16-69-6	4000	2000	96,43	14,1	11,8
СДН-16-84-6	5000	2500	96,9	13,8	11,5
СДН-16-104-6	6300	3150	97,22	14,6	13,1
600 rpm					
СДН-14-44-10	630	325	93,98	5,6	4,06
СДН-14-56-10	800	410	94,65	5,76	4,63
СДН-15-39-10	1000	511	94,68	7,66	5,38
СДН-15-49-10	1250	637	95,16	7,54	6,56
СДН-15-64-10	1600	812	95,78	7,79	6,99
СДН-16-54-10	2000	1010	95,66	10,7	8,68
СДН-16-71-10	2500	1265	96,22	10,9	8,46
СДН-16-86-10	3200	1651	96,58	11,6	10,5
СДН-17-59-10	4000	2010	96,67	12,9	12,7
СДН-17-76-10	5000	2510	97,06	14,6	11,7
СДН-17-94-10	6300	3150	97,24	17,1	14,4
СДН-18-71-10	8000	4000	96,94	22,3	20,1
СДН-18-91-10	10 000	5000	97,26	22,7	22,1

MAIN CONCLUSIONS AND RESULTS OF CHAPTER FOUR

1. *Optimization of the CRL in the ESS of a powerful industrial facility was carried out. For this purpose, a thorough analysis of the circuit-technical features of the facility was carried out, allowing for the creation of an adequate concept of the optimization process. The load analysis was carried out on a daily and monthly basis, and the characteristic coefficients for four significant units of the ESS were determined. The main findings of the study are related to the unsatisfactory load regime of the facilities and active power and the deteriorated indicators of the reactive substances of the load. It was found that the industrial facility is operated with deteriorated energy indicators and low $\cos\varphi$, a stable character within the limits of $\cos\varphi = 0,77 \div 0,86$.*

2. *The operation and parameters of the main facilities at the site – sources of reactive power (synchronous motors, power transformers, cable lines, asynchronous motors, capacitor banks) have been analyzed. A quantitative assessment of the generated reactive power has been made, and the active losses in the transfer of reactive energy have also been determined. The main technical characteristics of the specified facilities have been marked and their participation in the reactive power balance of the site has been predicted. A finding has been made about the existence of real possibilities for using SD as compensators, carried out on the basis of a preliminary assessment of the operability, functionality and possibilities for optimal operation of these facilities.*
3. *An optimization problem is defined according to the criterion "**Minimum of the reduced annual costs**" and four restrictive conditions. The extremum of the objective function is determined using the Lagrange method. Operational and economic characteristics of CRL with SD are determined, with power losses represented as a polynomial of the second degree with three terms - the first is proportional to Q , the second to $Q_0 \cdot Q$ and the third to Q^2 . An objective function for PGR is composed, consisting of three components (3_0 , 3_1 и 3_2), presented in tabular form for different types of SD. In a similar way, the objective function for KB is defined, with PGRs represented as a polynomial of the first degree. A verbal definition of the optimization problem is formulated as follows: "To determine which SDs and to what extent to use CRL and what economically feasible assessment can be made of the option for joint CRL of SD and KB." The synthesized methodology for optimizing reactive powers is maximally adapted to the capabilities of the circuit-technical data of the site and is adapted for the simultaneous use of SD and KB when conducting CRL.*
4. *The synthesized methodology was tested for the first and second sections of GPP 3 of the studied site. The solution of the optimization task requires performing a joint CRL at the medium voltage level using SD and at the low voltage level using KB. The results obtained confirm the operability of the proposed optimization approach in real conditions of operation of industrial sites. The technical and economic efficiency of the presented methodology has been proven and the possibility of its multiplication in similar industrial sites has been justified.*

GENERAL CONCLUSIONS AND RESULTS OF THE DISSERTATION

The work analyzes in detail conventional and highly innovative settings for CRL. Currently, the first type of compensation methods is widely used in the country's industry, due to its simplicity in application and operation, which is the reason for these methods to be studied in depth. Such are the preferences of the majority of companies, dictated mainly by economic considerations. In addition, the methodology of the regulatory framework is adapted to the construction of this type of CRL, which makes

it preferred from this point of view. The grounds for the application of innovative technical solutions based on intelligent technical settings are also highlighted. Highly effective circuit solutions are recommended for implementation, built as adaptive filter-compensating systems, minimizing several negative energy disturbances simultaneously. It is indicated that this approach has no alternative in the construction of intelligent power supply systems.

The CRL is considered in the conditions of nonlinear and unbalanced systems, the assessment of which is presented using various power theories depending on the system load. The relative relationship between the CRL and the quality of EE is proven using analytical dependencies, adequately reflecting the energy impact of its load on the PCEE and reactive powers, which increases the probability of realizing optimal CRL. The work confirms the applicability of such a complex approach to achieving effective CRL in various powerful industrial facilities operating under conditions of highly variable load, and also introducing significant disturbances to the quality of EE in the EES. Methodological statements for synthesizing FCCs have been developed, which take into account and assess the probability of resonance phenomena and contribute to their minimization. The purpose of the presented methodologies is to characterize and clarify the possibilities for implementing more complex and non-specific approaches for CRL in the existing wide variety of consumers in the electrical system, operating in asymmetric and non-sinusoidal modes and large load dynamics.

Using the developed methodology according to the criterion "Electricity efficiency", an instrumental study was conducted on the CRL in a large industrial facility with strongly pronounced nonlinear and unbalanced modes at two load levels. The feasibility of compensation was proven even at low loads, since the registered power losses from the inactive power substances (N, S0 and D) are comparable to those caused by the active power P. Inefficient operation of the existing CRL system was established, confirmed also with the help of diagnostic tests conducted using infrared thermography. In this regard, a new approach to CRL was proposed by managing the compensating powers according to the criterion "Direction and magnitude of reactive power", applying anti-resonance protection, implementing sequential active filters and building SCADA for monitoring, control and management of power processes. The forecast is that these measures will provide electricity savings within the range of (3÷4)% of total consumption with a payback period of the facilities (3÷5) years.

The research process has proven the influence of the load on the energy characteristics of the facility, related to the CRL. Three-phase, power-weighted indicators have been determined and a comparative analysis has been made with conventional, unweighted indicators. The degree of reduction in the direction of decreasing the values of the weighted indicators has been determined and it has been proposed that the necessary compensating power QK be calculated using the power factor PF, and not by $\cos\varphi$. When determining PF, the developed methodological guidelines should be applied, and the power-weighted indicators should also be used. The latter must be used when determining the overload of the FCS.

In a large industrial facility in the chemical industry, an analysis of the circuit-technical features was made and the energy characteristics of the ESS were studied with the aim of creating an adequate concept for the CRL. An unsatisfactory load regime of the facility and operation with low $\cos\varphi$ were established. The sources of reactive power and their operational characteristics were analyzed and their participation in the balance of the reactive powers of the facility was predicted. A finding was made that there are real possibilities for using SD in the CRL process, carried out on the basis of a preliminary assessment of the operability, functionality and possibilities for optimal operation of these facilities. Operational and economic characteristics of the CRL with SD were determined, with the power losses being presented as a second-degree polynomial with three terms, proportional to Q , $Q_0 \cdot Q$ and Q^2 respectively.

An optimization problem was defined according to the criterion "Minimum of PGR" and four restrictive conditions. An objective function for the PGR of the SD was compiled, representing a polynomial of the second degree with respect to Q . An objective function for the KB was defined in a similar way, with the PGR representing a polynomial of the first degree with respect to Q . The synthesized methodology for the GPP3 of the site was tested, as the solution of the optimization problem requires the implementation of a joint CRL of the MV using the SD 6.3kV and of the LV using the KB 0.4kV. The proposed optimization approach has high workability and proven technical and economic efficiency and can be multiplied in other industrial sites..

C. AUTHOR'S REFERENCE ON THE CONTRIBUTIONS OF THE DEVELOPMENT

SCIENTIFIC CONTRIBUTIONS

1. An innovative theoretical formulation has been formulated based on the criteria “Electricity efficiency” with the application of a differentiated approach for determining the components of active losses from inactive power substances (N , S_o and D) in asymmetric and non-sinusoidal modes. The methodology has been tested in a power facility when studying the efficiency of the CRL in operating conditions.
2. A methodological statement has been formulated for determining three-phase, weighted indicators relative to power, which with a high degree of adequacy, reliability and identity are appropriate to use in calculating the power factor PF and in determining the overload of the FCS from the input. The statement has been tested for four levels of the three-phase full power of the studied object S_{zp} , and reduced three-phase weighted coefficients have been determined, compared to the traditionally used ones.

SCIENTIFIC - APPLIED CONTRIBUTIONS

1. Practical-applied settings for the CRL of powerful popular consumers (electric arc furnaces, industrial electronic converters, rolling mills, third-class consumers in terms of EMC) are presented, introducing significant disturbances into the ESS of industrial facilities - generation of inrush current, imbalance of current and voltages, shock loads, etc. The probability of occurrence of resonance phenomena in the case of uncalculated CRL and the means for suppressing these negative phenomena are analyzed. In a practical-applied aspect, methodological guidelines for calculating and synthesizing passive and active type PKUs are developed.
2. The conducted studies on CRT give grounds to claim that there is equivalence in the implementation of this process under different load conditions. The studies have established that the coefficient of additional losses in asymmetric and non-sinusoidal modes at reduced load K_D is about 20% higher than that at normal load and this is another fact in support of the need to apply CRT at reduced load.
3. The optimization of the CRL in the ESS of a powerful industrial facility in the chemical industry according to the criterion “Minimum of PGR” represents an implemented technical solution of a joint CRL with SD and KB, applied at two voltage levels - MV and LV. The optimization task makes it possible to determine the number and power of SD and to predict to what extent the use of KB is economically feasible.

PUBLICATIONS OF THE AUTHOR RELATED TO THE DISSERTATION

1. Iliev I., Petrov P., Delcheva D., Optimal distribution and location of compensating capacities in a9999n international aspect Energy Forum 24-27 June 2025., Sofia. ISSN 1313-2962, pp. 525– 535
2. Petrov P., Hydroelectric power plants - a main component of modern energy systems Energy Forum 24-27 June 2025., Sofia. ISSN 1313-2962, pp. 570– 582
3. Iliev I., Petrov P., Determining the dissipation zone of an electrical load center Energy Forum 24-27 June 2025., Sofia. ISSN 1313-2962, pp. 561– 569
4. Iliev I., Petrov P., Determining the orientation of the coordinate axes and constructing the dissipation zone of the center of electrical loads Energy Forum 24-27 June 2025., Sofia. ISSN 1313-2962, pp. 552– 560
5. Iliev I., Petrov P., Analysis of EEF of pumping stations Energy Forum 24-27 June 2025., Sofia. ISSN 1313-2962, pp. 544– 551

Author: Petar Ivanov Petrov

E-mail: p_petrov1977@abv.bg

Title: Influence of load on reactive power in asymmetric and non-sinusoidal regimes